Dalton Transactions

Hexafluoroantimony (V) salts of the cationic Ti(IV) fluoride non metallocene complexes $[TiF_3(MeCN)_3]^+$ and $[TiF_2L]^{2+}$ (L = 15-Crown-5 and 18-Crown-6). Preparation, characterization and thermodynamic stability.

Andreas Decken,[‡a] Evgeny G. Ilyin,[b] H. Donald Brooke Jenkins*[†c],Grigori B. Nikiforov,[a] Jack Passmore*[a]

Supplemental material.

1. Details of the cationic – anionic contacts found in complex [1].

Table 1

Bond	distance, Å	Bond valence, v.u. [1]	H – F contact	Distance, Å*
Sb-F(4)	1.815(7)	0.95	F5-H4b	2.837
Sb-F(6)	1.815(7)	0.95	F5-H6a	2.761
Sb-F(9)	1.835(9)	0.90	F7-H2b	2.549
Sb-F(7)	1.836(7)	0.90	F7-H2c	2.938
Sb-F(8)	1.836(7)	0.84	F8-H4a	2.873
Sb-F(5)	1.861(6)	0.80	F8-H4c	2.786
			F8-H6a	2.658
			F9-H4a	2.707
			F9-H6c	2.763

* C-H distance has fixed length 0.98 Å

The antimony fluorine distances are typical for those found in the isolated $[SbF_6]^-$ anion [2]. The $[SbF_6^-]$ anion is surrounded by the hydrogen atoms of the acetonitrile molecules. Those H – F non bonded contact distances which are less than 3Å are listed in Table 1. The shortest contacts are comparable with the sum of the Van der Waals radii of hydrogen and fluorine 2.7 Å [3(a)] and the sum of the Sb-F bond valences is 5.34, it is therefore concluded that the *face*-$[TiF_3(MeCN)_3]^+$ cation interacts only very weakly with the $[SbF_6]^-$ anion in [**1**].

2. Details of the cationic – anionic contacts in complexes [2] and [3].

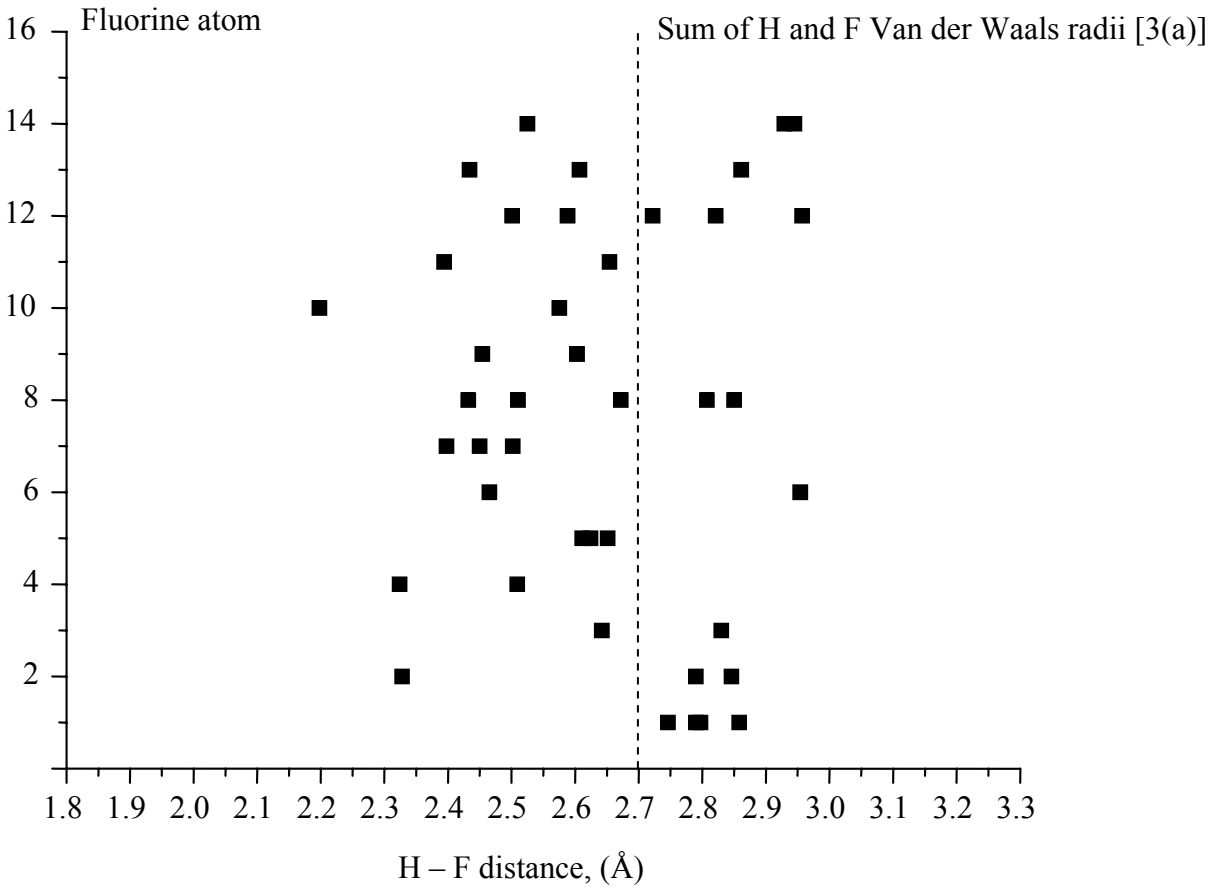

Figure 1. H – F distances between the hydrogen atoms of 15-Crown-5 and fluorine atoms of $[SbF_6]^-$ in $[TiF_2(15\text{-Crown-5})][SbF_6]_2$ **[2],** details of 41 contacts at less than 3 Å apart are included in the plot, the C-H distance has a fixed length equal to 0.98 Å.

The shortest contacts are those of: F(4) - H(15B) 2.324 Å, F(7) – H(2A) 2.450 Å, F(10) – H(6A) 2.198 Å and F(11) – H(9A) 2.394 Å suggesting weak H-F bonding exists in the solid **[2]**, however the Raman bands found in **[1]** at 279, 647 cm^{-1} and in **[2]** at 281, 647 cm^{-1} are identical. The shape and position of ^{19}F NMR resonances of $[SbF_6]$ in **[1]** and **[2]** are identical showing that no cation - anion interaction arises in solution.

Table 2. Sb-F distances in complex **[2]**.

Bond	distance, Å	Bond valence, v.u.
Sb(1)-F(6)	1.847(3)	0.87
Sb(1)-F(4)	1.859(2)	0.85
Sb(1)-F(8)	1.865(2)	0.83
Sb(1)-F(5)	1.871(2)	0.82
Sb(1)-F(7)	1.871(3)	0.82
Sb(1)-F(3)	1.875(3)	0.81
Sb(2)-F(9)	1.816(3)	0.95
Sb(2)-F(13)	1.834(3)	0.91
Sb(2)-F(10)	1.853(3)	0.86
Sb(2)-F(11)	1.854(3)	0.86
Sb(2)-F(14)	1.858(3)	0.85
Sb(2)-F(12)	1.873(3)	0.81

The antimony fluorine distances in **[2]** and **[3]** are typical for those found in the isolated $[SbF_6]^-$ anion [2] and are slightly longer than those found in **[1]** due to stronger cation anion contacts in **[2]** (and **[3]**). The sums of v.u. around Sb(1) (= 5.00v.u.) and Sb(2) (= 5.24v.u.) indicate that the $[Sb(1)F_6]^-$ anion is the more strongly interacting of the two with the *trans* - $[TiF_2(15\text{-Crown-5})]^{2+}$ cation.

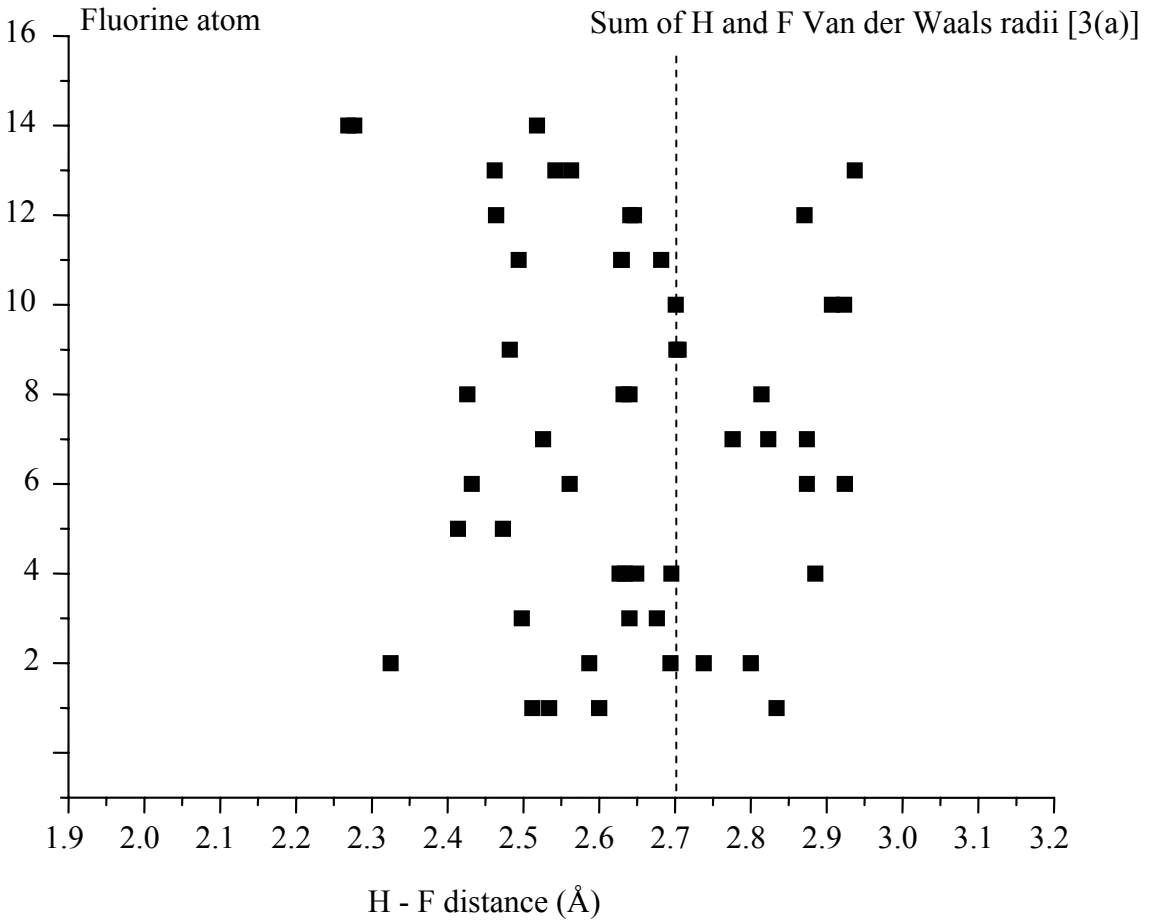

Figure 2. H – F distances between the hydrogen atoms of 18-Crown-6 and fluorine atoms of $[SbF_6]^-$ in $[TiF_2(18\text{-Crown-6})][SbF_6]_2$ **[3]**, details of the 52 contacts at distances less than 3 Å are represented in the figure above, the C-H distance has a fixed length of 0.98 Å.

The shortest H-F contacts in **[3]** are seen to be**:** F(14)-H18(A) 2.277 Å, F(5) – H(11B) 2.473 Å, F(6) – H(18A) 2.432 Å and F(8) – H(12B) 2.426 Å and are fairly close to those seen in **[2]** and suggest weak H-F bonding exists in the solid **[3]**, while Raman bands in **[1]** at 279, 647 cm^{-1}, in **[2]** at 281, 647 cm^{-1} and in **[3]** at 282, 647 cm^{-1} are similar. The shape and position of ^{19}F NMR resonances of $[SbF_6]$ in **[1]**, **[2]** and **[3]** are identical showing no (or very minimal) cation - anion interaction exists in solution.

Table 3 Sb-F distances in [3].

Bond	distance, Å	Bond valence, v.u.
Sb(1)-F(3)	1.865(2)	0.83
Sb(1)-F(5)	1.873(2)	0.81
Sb(1)-F(6)	1.875(2)	0.81
Sb(1)-F(4)	1.875(2)	0.81
Sb(1)-F(7)	1.881(2)	0.80
Sb(1)-F(8)	1.882(2)	0.80
Sb(2)-F(9)	1.854(2)	0.86
Sb(2)-F(10)	1.862(3)	0.84
Sb(2)-F(11)	1.863(2)	0.84
Sb(2)-F(12)	1.866(2)	0.83
Sb(2)-F(13)	1.876(2)	0.81
Sb(2)-F(14)	1.879(2)	0.80

Antimony fluorine distances in complex **[3]** are slightly longer to those found in **[1]** due to the existence of stronger cation anion contacts in **[3]** as compared to **[1]**. The sum of v.u. around Sb(1) (= 4.86v.u.) and Sb(2) (= 4.98 v.u.) show that the $[Sb(1)F_6]^-$ anion in **[3]** to be the more strongly interacting anion with the *trans* - $[TiF_2(15\text{-Crown-5})]^{2+}$ cation, as was found in the case of complex **[2]**.

4. IR 4000-350cm^{-1} and Raman 4000-120 cm^{-1} spectra of complexes: [1] (Figure 3 [4000 – 350 cm^{-1}], Figure 4 [4000 – 120 cm^{-1}]), **[2]** (Figure 5 [1500 – 400 cm^{-1}], Figure 6 [3500 – 120 cm^{-1}]) and **[3]** (Figure 7 [1500 – 400 cm^{-1}], Figure 8 [4000 – 120 cm^{-1}])**,and assignments** (Table 4 and 5)

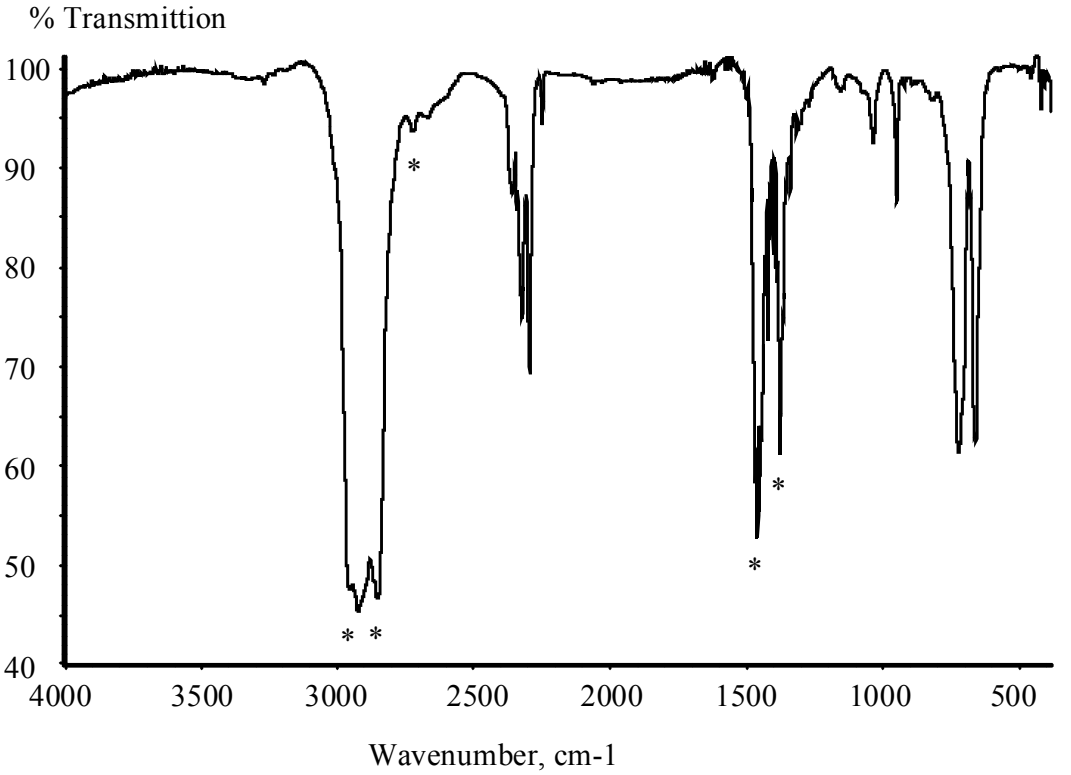

Figure 3.

IR spectrum of **[1]**, Nujol, KBr, * (Nujol).

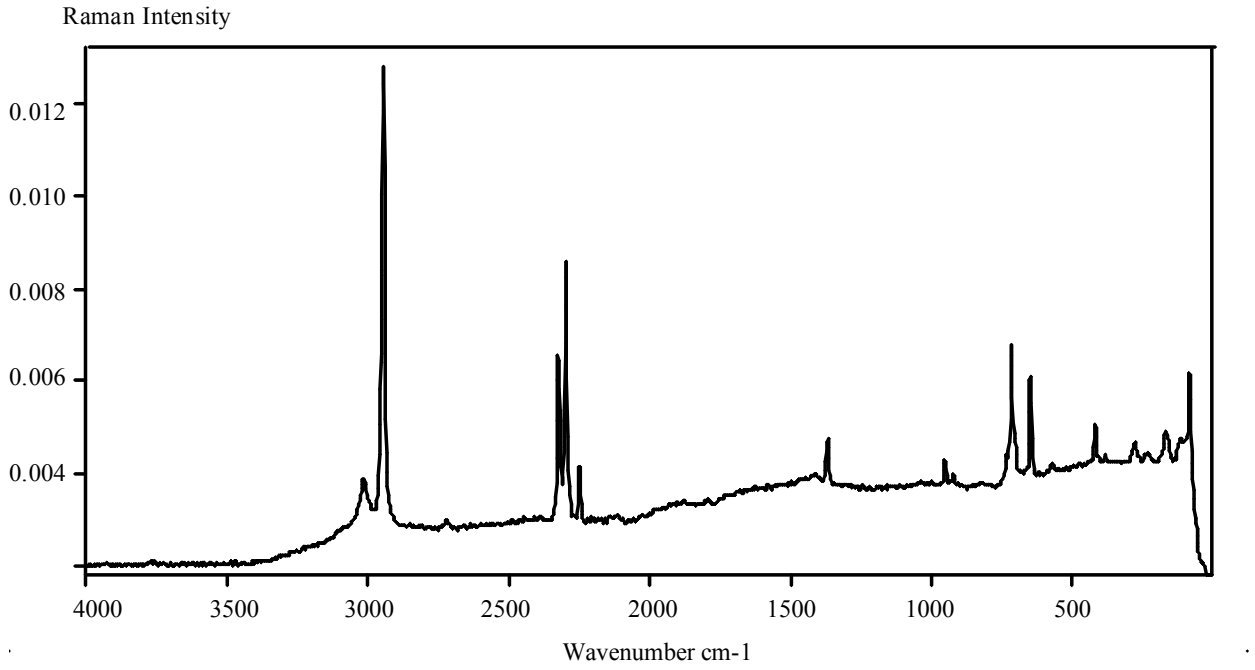

Figure 4.

Raman spectrum of $[TiF_3(MeCN)_3][SbF_6]$ **[1]**, resolution 4, 1000 scans.

Table 4.

Assignment of the absorption bands in the IR spectrum of $[TiF_3(MeCN)_3][SbF_6]\cdot MeCN$ **[1]**

Observed frequency and relative intensity ν (cm^{-1})		Assignment	MeCN [4]	$[SbF_6]^-$ [5](O_h)
IR	Raman			
	115 (br, w)	TiF_3N_3 deformation		
	169 (br, m)	TiF_3N_3 deformation		
	229 (br, w)	Ti-N		
	279 (m)			$\nu_5(F_{2g})$
	383 (w)	MeCN in lattice	380 $\nu_8(E)$ (N≡C-C)	
	419 (s)	(N≡C-C) coordinated MeCN		
	572 (w)			$\nu_2(E_g)$
	647 (vs)			$\nu_1(A_{1g})$
659 (br, vs)	660 (w)			$\nu_3(F_{1u})$
710-740 (br, vs)	716 (vs)	$\nu_s(TiF_3)$		
	734 (w, sh)	ν_{as} (TiF_3)		
920 (w)	920 (w)	MeCN in lattice	918 (A_1) ν_4(C-C), ν_4(C-N)	
948 (s)	951 (w)	ν(C-C) + ν(C-N), coordinated MeCN		
1036 (s)	1036 (w)	$\nu(CH_3)$ rocking, coordinated MeCN		
1151 (w)		MeCN in lattice	1124 (E) $\nu_7(CH_3)$ rocking	
1368 (m)	1367 (m)	$\nu(CH_3)$ coordinated MeCN		
1376(m)		MeCN in lattice	1376 (A_1) $\nu_3(CH_3)$	
	1413 (w)	$\nu(CH_3)$ coordinated MeCN		

2250 (m)	2250 (w)	MeCN in lattice	2249 (A_1) ν_2(C≡N)	
2295 (vs)	2296 (vs)	ν(C≡N), coordinated MeCN		
2323 (s)	2323 (s)	ν(C≡N), coordinated MeCN		
2359 (m)		ν(C≡N), coordinated MeCN		
	2722 (w)	$2\nu_3(CH_3)$	2725 (A_1) $2\nu_3(CH_3)$	
	2945 (vs)	ν(C-H) lattice MeCN	2942 (A_1), ν_1(C-H)	
3014 (w, br)	3014 (w, br)	ν(C-H)lattice MeCN	2999 (E) ν_5(C-H)	

Table 5.

Assignments of the vibrational spectra of $[TiF_2(15\text{-Crown-5})][SbF_6]_2$ **[2]** and $[TiF_2(18\text{-Crown-6})][SbF_6]_2$ **[3]**.

Observed frequency and relative intensity ν (cm^{-1})				Assignment		15-Crown-5*	18-Crown-6*	$[SbF_6]^-$ (O_h)†
2		**3**		**2**	**3**			
IR	Raman	IR	Raman					
	139 (w)		148 (w)	Sceletal deformations of 15-Cr-5 100-700 cm^{-1}	Sceletal deformations of 18-Cr-6 100-700 cm^{-1}		134 (w), (R)	
	239 (w)		190 (w)				232 (w), (R)	
	256 (w)		256 (m)				271 (m), (R)	
	281 (s)		282 (s)				276 (s), (R)	282 (R) $\nu_5(F_{2g})$
	311 (w)		318 (m)			303 (m), (R)	320 (m), (R)	
			358 (w)				352 (m), (R)	
396 (w)	395 (s)		391 (w)	ν_s (Ti-O)	ν (Ti-O)			
			418 (m)		ν (Ti-O)		415 (vs), (R)	
		422 (s)			δ (O-Ti-O)			
		432 (s)			δ (O-Ti-O)			
453 (s)		463 (m)		δ_e (O-Ti-O)			463 (w), (IR)	
		490 (w)		Sceletal deformations of 15-Cr-5	Sceletal deformations of 18-Cr-6			
	502 (w)	506 (m)				522 (w), (R)	526 (m), (IR)	
536 (w)	538 (w)	538 (w)				540(w), (IR, R)	537 (m), (IR)	
		544 (m)					548 (m), (R)	
		569 (w)					568 (w), (IR)	
576 (w)	573 (m)	578 (sh)	575 (w)				580 (s), (R)	575 (IR) $\nu_2(E_g)$
		586 (w)					582 (m), (IR)	
597 (sh)	599 (s)		599 (s)	ν_s (Ti-F)	ν_s (Ti-F)			
		616 (m)				617 (w) (IR)		
647 (vs, sh)	647 (vs)		647 (vs)					652 (R) $\nu_1(A_{1g})$
660 (vs, br)		659 (vs, br)						655 (IR) $\nu_3(F_{1u})$
		677 (w)					670 (m), (IR)	
695 (vs, br)		697 (vs)		ν_{as} (Ti-F)	ν_{as} (Ti-F)			
			707 (w)					
		762 (s)	762 (w)					

		789 (s)	790 (w)					
			799 (w)	Sceletal	Sceletal		824 (s), (R)	
		810 (s)		deformations	deformations		827 (m), (IR)	
827 (vs)		822 (s)		and	and	831 (s), (IR, R)	833 (m), (IR, R)	
			865 (w)				866 (s), (R)	
		868 (w)		torsions	torsions	856 (w), (IR, R)	861 (s), (IR)	
		882 (m)		of 15-Cr-5	of 18-Cr-6		886 (w), (IR)	
			885 (w)				892 (s), (R)	
892 (w)	898 (w)	913 (s)		700-1200	700-1200	910 (s), (R)		
			929 (w)				939 (w), (R)	
	927 (w)	929 (s)		cm^{-1}	cm^{-1}	932 (s) (IR, R)	945 (s), (IR)	
		946 (s)						
	967 (w)					970 (m), (R)		
984 (vs)	976 (w)	976 (s)				983 (m), (IR, R)	963 (s), (IR)	
998 (s)	992 (w)	991 (s)	995 (w)			1010 (m), (R)	993 (s), (IR, R)	
		1019 (m)	1018 (w)					
		1025 (m)						
		1041 (s)					1047 (m), (IR, R)	
		1054 (s)	1056 (w)				1063 (m), (IR, R)	
1061 (vs, br)	1063 (w)	1067 (s)				1040 (m), (IR, R)	1076 (m), (IR)	
	1081 (w)	1081 (w)	1078 (w)				1085 (m), (R)	
	1105 (w)	1108 (w)					1108 (vs), (IR)	
1119 (w)	1119 (w)	1124 (m)				1092 (m), (IR, R)	1129 (vs), (IR, R)	
1133 (m)	1134 (w)	1140 (m)	1141(w)			1120 (m), (IR, R)	1140 (sh), (IR)	
		1153 (m)					1154 (m), (IR)	
	1234 (w)	1227 (w)	1231 (m)			1240 (s), (R)	1235 (m), (IR, R)	
1242 (s)		1239 (m)				1250 (s), (IR)	1237 (m) (IR)	
	1250 (w)	1250 (w)		methylene	methylene		1248 (s), (IR)	
1257 (m)		1256 (m)	1257 (m)	twisting,	twisting,		1259 (s), (IR, R)	
1269 (s)	1269 (w)	1266 (m)	1269 (m)	wagging,	wagging,	1260 (sh), (R)	1275 (s), (IR, R)	
1276 (s)	1280 (w)	1284 (m)	1286 (w)	internal	internal	1294 (s), (IR)	1286 (m) (IR)	
		1299 (m)		deformation	deformation		1296 (s) (IR, R)	
		1325 (m)	1325 (m)	vibrations	vibrations			
		1335 (w)		of 15-Cr-5	of 18-Cr-6		1335 (w), (IR)	
		1346 (w)		1200-1500	1200-1500		1352 (s), (IR)	
	1372 (w)	1366 (w)	1364 (m)	cm^{-1}	cm^{-1}	1360 (s), (IR,R)	1369 (s), (R)	
			1443 (m)				1446 (s), (R)	

	1401 (w)					1390 (s), (R)		
			1460 (m)				1465 (s), (R)	
	1471 (m)		1471 (s)			1452 (m, br), (R)	1476 (s), (R)	
			1495 (w)				1492 (s), (R)	
2210 (m)		2210 (m)						
2275 (m)		2275 (m)						
	2701 (w)						2704 (w), (R)	
	2737 (w)		2775 (w)	*v*(C-H)	*v*(C-H)		2764 (w), (R)	
	2796 (w)		2815 (w)	of 15-Cr-5	of 18-Cr-6		2810 (m), (R)	
	2849 (m)		2841 (w)	2700-3100	2700-3100		2842 (s), (R)	
			2869 (w)	cm^{-1}	cm^{-1}		2874 (vs), (R)	
	2882 (m)		2890 (w)			2870 (vs)	2896 (vs), (R)	
	2911 (m)		2910 (w)			2909 (vs)		
	2935 (m)		2931 (m)				2950 (vs), (R)	
	2983 (vs)		2978 (vs)				2996 (vs), (R)	
	3023 (vs)		3021 (s)					
			3035 (s)					
			3068 (w)					

* 18-Crown-6 crystallizes in conformations possessing D_{3d} and C_i symmetry, for assignment of 15-Crown-5 and 18-Crown-6 Raman spectra see [**Error! Bookmark not defined.**, 6], IR [6(a,c)]. † vibrations of $[SbF_6]^-$ anion are taken from ref [5] for $[N_5][SbF_6]$ containing a separate $[SbF_6]^-$ anion.

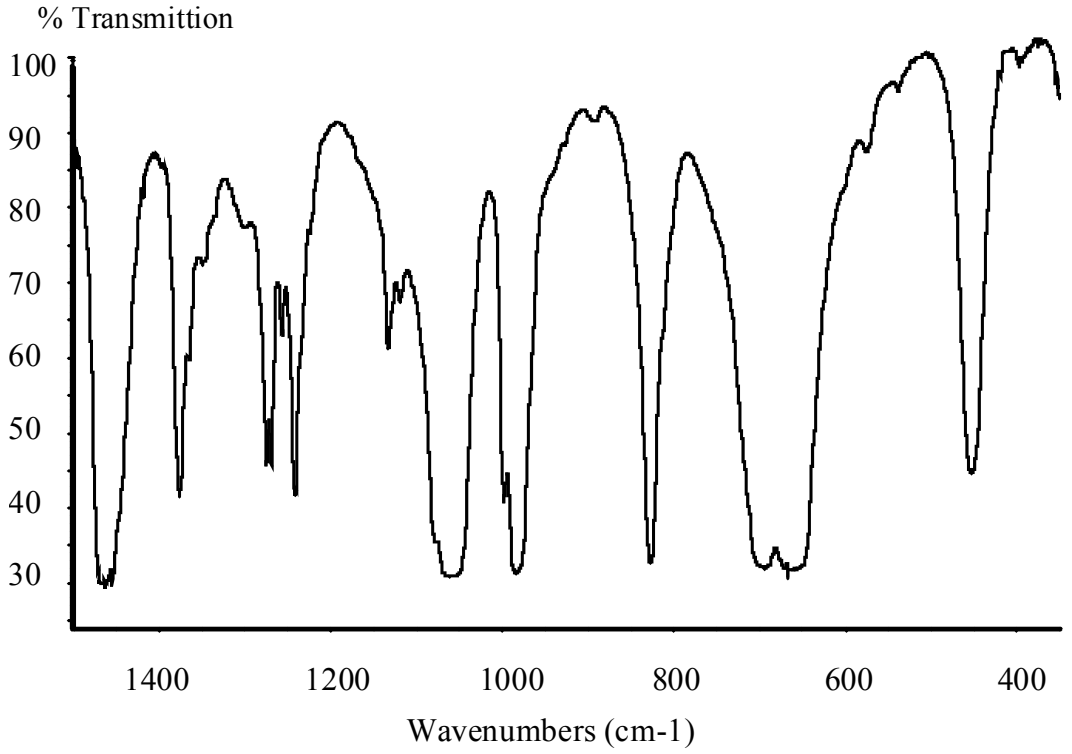

Figure 5.

IR spectrum of the *trans* - $[TiF_2(15\text{-Crown-5})][SbF_6]_2$ (**2**), Nujol, KBr, * (Nujol). Range: 1500 - 4000 cm^{-1}.

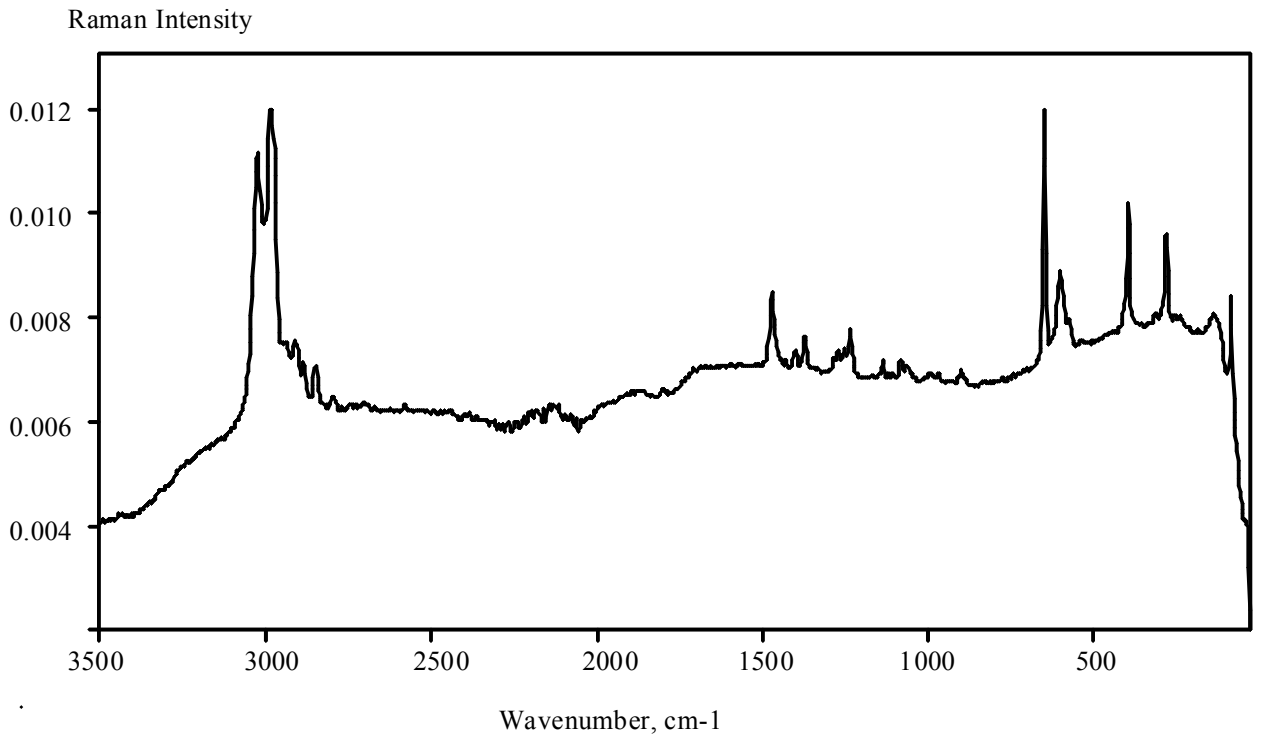

Figure 6.

Raman spectrum of the $[TiF_2(15\text{-Crown-5})][SbF_6]_2$ **[2]**, resolution 4, 1000 scans

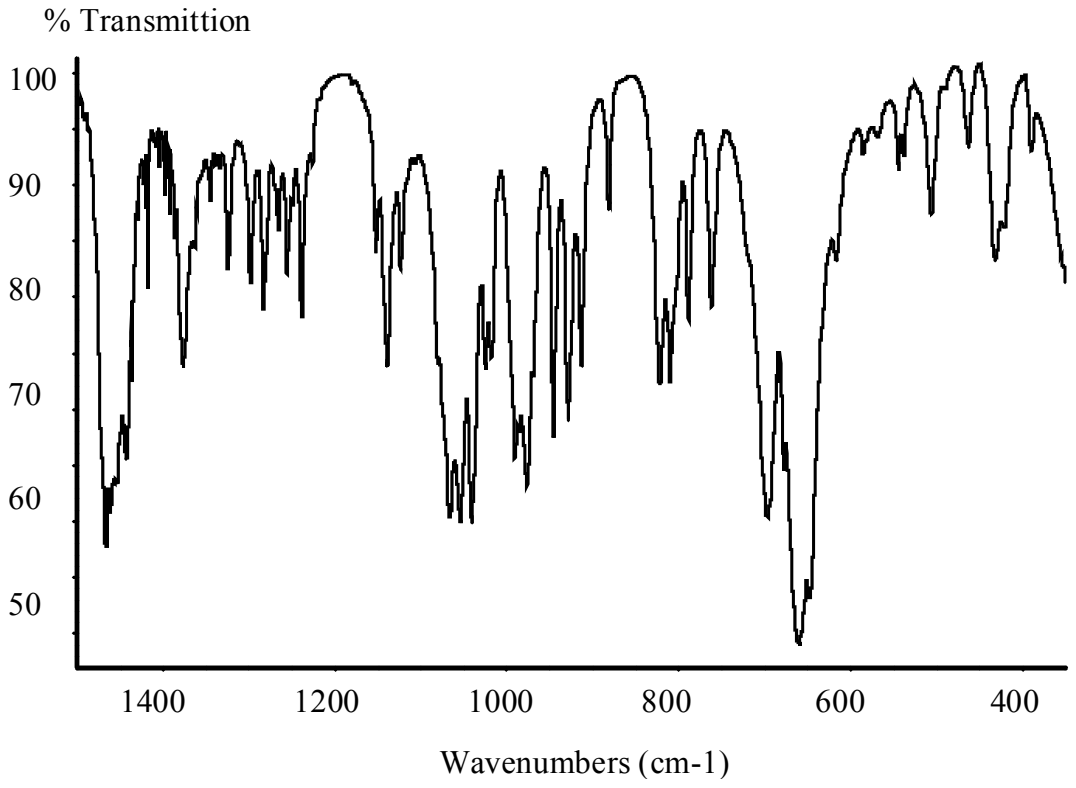

Figure 7.

IR spectrum of the $[TiF_2(18\text{-Crown-6})][SbF_6]_2$ [**3**]. Area 1500 - 4000 cm^{-1} contained signals of nujol only.

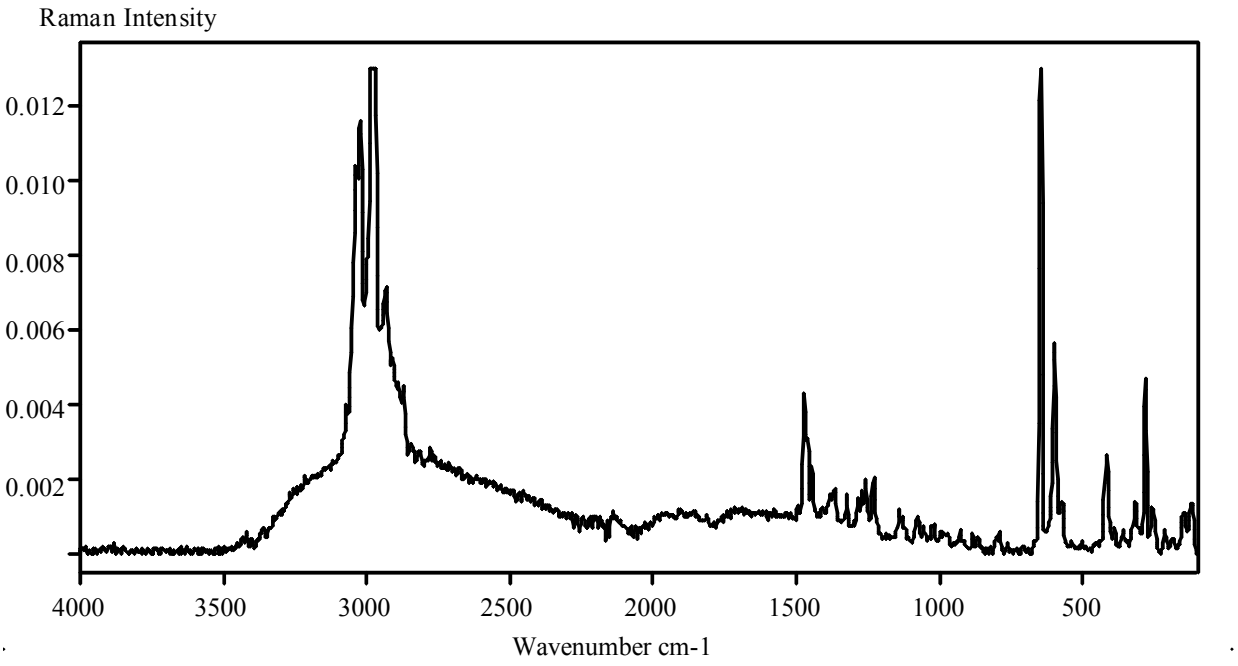

Figure 8.

Raman spectrum of $[TiF_2(18\text{-Crown-6})][SbF_6]_2$ **[3]**, resolution 4, 1000 scans

5. Interaction of $[TiF_3(MeCN)_3][SbF_6]\cdot MeCN$ [1] and excess of Et_2O in MeCN.

The ^{19}F NMR spectrum of a solution of **[1]** in the mixture 75% MeCN and 25%Et_2O exhibits at r.t. a strong signal due to *face*-$[TiF_3(MeCN)_3]^+$, a broad exchange resonance at 317 ppm assigned to the mixed cationic complex containing Et_2O and MeCN, a resonance of the $[SbF_6]^-$ anion as well as weak broad resonance 207 ppm assigned to the $TiF_4(Et_2O)_2$ and a further weak signal at 238 ppm.

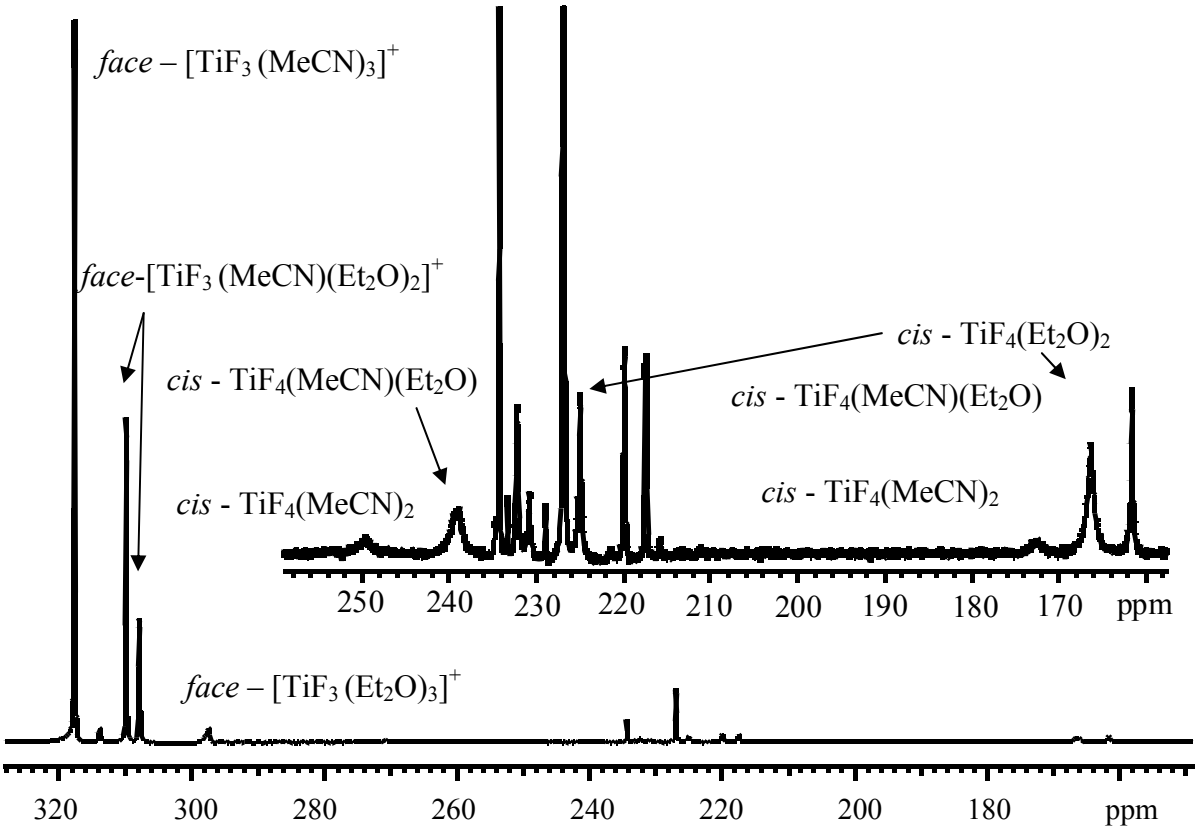

Figure 9.

^{19}F NMR spectrum of **[1]** in the mixture 0.25 mol. % Et_2O and 0.75 mol. % MeCN at -60 ºC. Spectrum is measured one day after preparation of solution.

Lowering the temperature reduces the exchange processes and narrows the resonances and allows one to observe separate lines of the *face*-$[TiF_3(MeCN)_{3-n}(Et_2O)_n]^+$ n = 0 - 3 complexes (Figure 9., Table 5 main text) at -60 ºC. The total relative intensity of the resonances assigned to the cationic complexes is reduced to 91% when measured 1 day after preparation of the solution.

The ^{19}F resonances at 250 and 173 ppm, 224.9 and 161.5 ppm and 229.5, 211.0, 162.3 ppm were attributed to the molecular adducts *cis*-$TiF_4(MeCN)_{2-n}(Et_2O)_n$ n = 0 - 2 according to previous work [7,8]. The total relative intensity of molecular complexes is 3% in the ^{19}F NMR spectrum when measured 1 day after preparation of solution.

The group of signals at δ_F 234.2, 232.2, 226.8, 219.8, 217.5 ppm do not belong to the cationic, molecular or oligomeric Ti(IV) fluoride complexes [7,8,9]. We propose that these lines belong to the mixed Ti(IV) fluoride complexes containing bridging and terminal $[OEt]^-$ groups which have resulted from cleavage of the C-O bond in Et_2O.

Formation of the $SbF_5(Et_2O)$ complex was detected by means of ^{19}F NMR (Fig.10). The resonance of $[SbF_6]^-$ -123 ppm with the fine structure due to coupling with ^{121}Sb I = 5/2 and ^{123}Sb I = 7/2 [10,11] overlaps with the signals δ_F –110.3, -120.1, -130.5 ppm of this species (Fig.10).

The proton spectrum of **[1]** in the mixture MeCN and Et_2O at -60 ºC shows several resonances assigned to the [OEt] group at 4.9 – 4.3 and 1.75-1.62 ppm as well as the resonances of the Et_2O, MeCN.

The color of the reaction mixture of **[1]** and Et_2O-MeCN changes from colorless to yellow, over time. The relative intensities of ^{19}F resonances of the cationic complexes decreased, while resonances of *cis*-$TiF_4(MeCN)_{2-n}(Et_2O)_n$ n = 0 - 2 and 218.5 ppm increased. The total relative intensity of the molecular complexes is 33% in the ^{19}F NMR spectrum as measured 3 weeks after preparation of solution, the resonance at 218.5 ppm has 62% relative intensity whilst the relative intensity of the cationic complexes *face*-$[TiF_3(MeCN)_{3-n}(Et_2O)_n]^+$ n = 0 - 3 is only 2%. Deposition of solid product was not observed from the reaction mixture, the residue obtained after evacuation of all volatile products under dynamic vacuum was yellow tar oil.

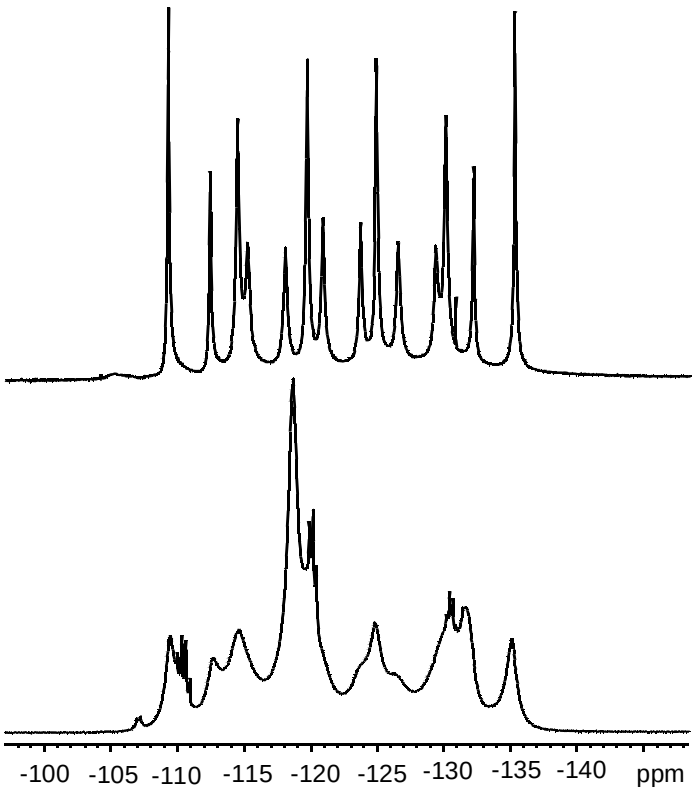

Figure 10.

Upper spectrum: ^{19}F NMR resonance of the $[SbF_6]^-$ anion in the NMR spectrum of **[1]** in MeCN, with the fine structure due to coupling with ^{121}Sb $I = 5/2$ and ^{123}Sb $I = 7/2$.
Lower spectrum: ^{19}F NMR resonances in spectrum of **[1]** in the mixture 0.25 mol. % Et_2O and 0.75 mol. % MeCN at -60 ºC, showing signal of $[SbF_6]^-$ anion overlapping with the resonances assigned to $SbF_5(Et_2O)$ of the antimony fluoride complex. Spectrum as measured one day after the preparation of solution.

NMR scale Experiment. Reaction of $[TiF_3(MeCN)_3][SbF_6]\cdot MeCN$ [1] and Et_2O in MeCN: Complex **[1]** (0.1 g, 0.2 mmol) was added to a 5 mm NMR tube and 0.3 ml (0.21g, 2.9 mmol) of Et_2O and 0.6 ml (0.47g, 11.4 mmol) of MeCN were added *via* vacuum line. A clear colorless solution was obtained by warming to r.t. The NMR spectra were measured the day after preparation. ^1H NMR (400 MHz, MeCN, -60 ºC), δ_H (ppm) = 4.9 (q, 2H, J = 7.1 Hz, CH_3CH_2O), 4.7 (q, 2H, J = 7.0 Hz, CH_3CH_2O), 4.6 (q, 2H, J = 6.5 Hz, CH_3CH_2O), 4.5 (br, CH_3CH_2O), 4.3 (q, 2H, J = 7.2 Hz, CH_3CH_2O), 3.6 (Et_2O solvent), 2.0 (MeCN solvent), 1.75

(t, 3H, J = 7.1 Hz, CH_3CH$_2$O), 1.73 (t, 3H, J = 6.0 Hz, CH_3CH$_2$O), 1.67 (t, 3H, J = 7.0 Hz, CH_3CH$_2$O), 1.62 (t, 3H, J = 7.0 Hz, CH_3CH$_2$O), 1.52 (t, 3H, J = 7.0 Hz, CH_3CH$_2$O), 1.50 (t, 3H, J = 7.2 Hz, CH_3CH$_2$O), ^{19}F NMR (MeCN, 25 ºC), δ_F (ppm) = 324.4 (br), 316.8 (br), 238.2 (br), 207.0 (br), ^{19}F NMR (MeCN, -60 ºC), δ_F (ppm) = 317.7 (s, 3F, *face*-[TiF_3(MeCN)$_3$]$^+$), 313.7 (br, 1F, *face*-[TiF_3(MeCN)$_2$(Et$_2$O)]$^+$), 309.8 (br, 2F *face*-[TiF_3(MeCN)(Et$_2$O)$_2$]$^+$), 307.8 (br, 1F *face*-[TiF_3(MeCN)(Et$_2$O)$_2$]$^+$), 297.9 (br, 3F *face*-[TiF_3(Et$_2$O)$_3$]$^+$), 270.7 (br), 250 (br, 2F *cis*-TiF_4(MeCN)$_2$), 239 (br, 1F *cis*-TiF_4(MeCN)(Et$_2$O)), 234.2, 232.2 (br, 1F *cis*-TiF_4(MeCN)(Et$_2$O)), 226.8 (br), 224.8 (br, 2F *cis*-TiF$_4$(Et$_2$O)$_2$), 219.8(br), 217.4(br), 173 (br, 2F *cis*-TiF_4(MeCN)$_2$), 166.3 (br, 2F *cis*-TiF_4(MeCN)(Et$_2$O)), 161.5 (br, 2F *cis*-TiF$_4$(Et$_2$O)$_2$), -107.1 (d, 4F, J = 98.4 Hz, SbF$_5$(Et$_2$O)), -110.4 (q, J = 103.8 Hz), -120.5 (t, J = 113.7 Hz), -123.3 (m, 6F, [SbF_6]$^-$ J(^{121}Sb-^{19}F) 1944 Hz, J(^{123}Sb-^{19}F) 1020 Hz), -130.6 (q, J = 95.4 Hz).

6. Reaction of [1] with excess of THF in MeCN.

The ^{19}F NMR spectrum of a solution of **[1]** together with 2 moles of THF in MeCN displays the resonances of *face*-[TiF$_3$(MeCN)$_{3-n}$(THF)$_n$]$^+$ n = 0 - 3, *cis*-TiF$_4$(THF)$_2$ (Figure 11.) and decomposition products probably resulting from C-O bond cleavage in THF. The total relative intensity of the cations is 38%, of the molecular complex is 19% and for a resonance at 217.6 ppm is 41%, measured 2 hours after preparation of solution at -40°C. The latter resonance (217.6 ppm) is assigned to the same decomposition products that have a similar chemical shift in a mixture of **[1]** and Et$_2$O-MeCN, suggesting that they could be alkoxide complexes with [OEt], [OBu] ligands, or titanium complexes with a bridging oxygen atom. Addition of excess THF leads to formation of the *face*-[TiF$_3$(THF)$_3$]$^+$ (14%), *cis*-TiF$_4$(THF)$_2$ (44%) and decomposition products exhibiting resonances at 218.1, 181.4, 167.6 ppm (42%), as

measured 2 hours after preparation of the solution containing **[1]** and 10 moles of THF in MeCN at -40°C.

Relative intensity of the cationic complexes decreased with time while resonances of *cis*-$TiF_4(THF)_2$ increased. Finally, the molecular complex is the major product in solution with a relative concentration close to 54% (**[1]** with 2 mol. of THF) and 70% (**[1]** with 10 mol. of THF) measured at -40 ºC, 10 days after preparation (Figure 11.).

Formation of the mixed antimony fluoride complexes ($SbF_5(THF)$) was detected by means of ^{19}F NMR (Fig.12). The resonance of $[SbF_6]^-$ -121 ppm overlaps with the resonances δ_F -109, -117 ppm assigned to the $SbF_5(THF)$ adduct (Figure 12.).

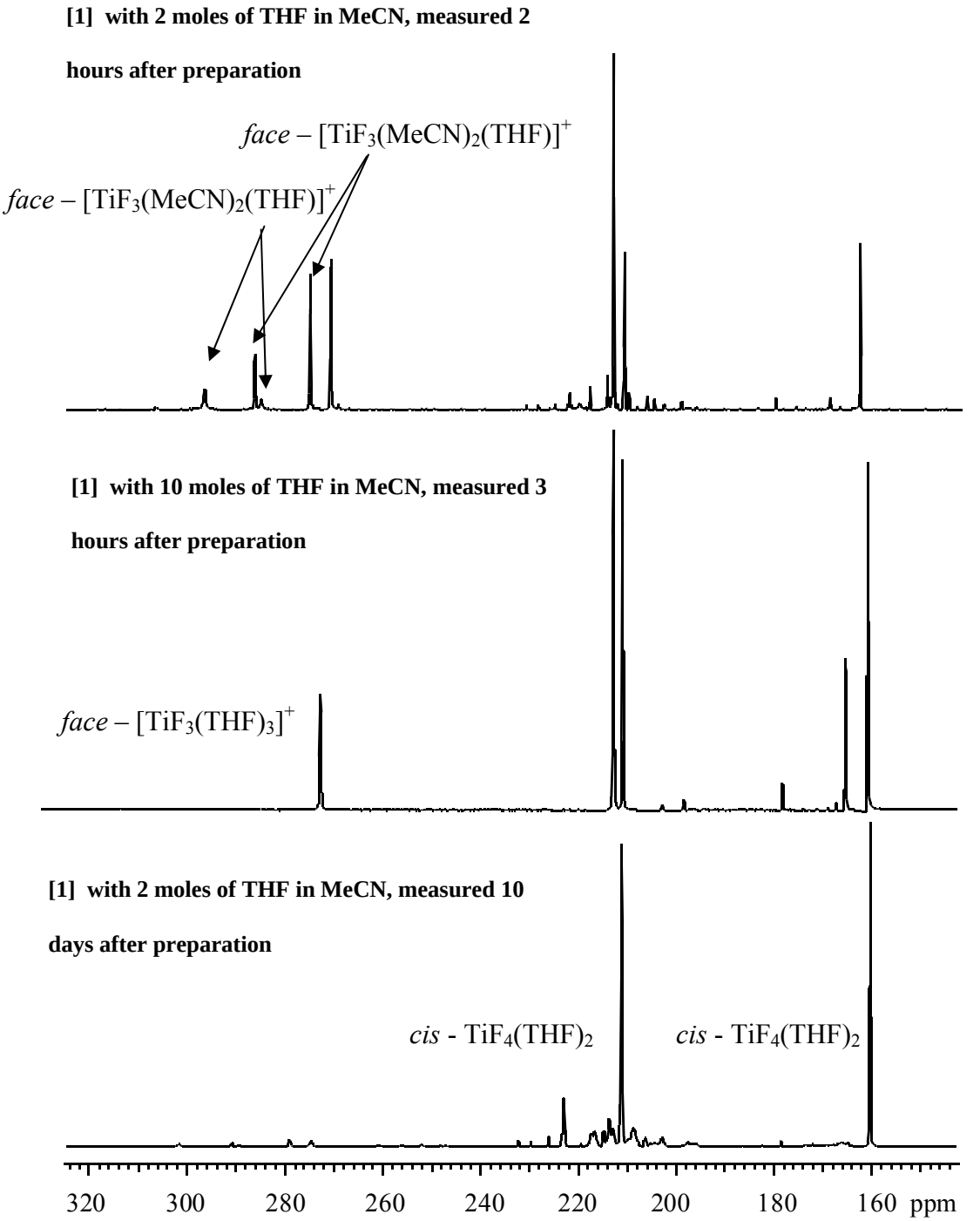

Figure 11.

^{19}F NMR spectrum of **[1]** with THF in MeCN at -40 ºC measured 2, 3 hours and 10 days after preparation.

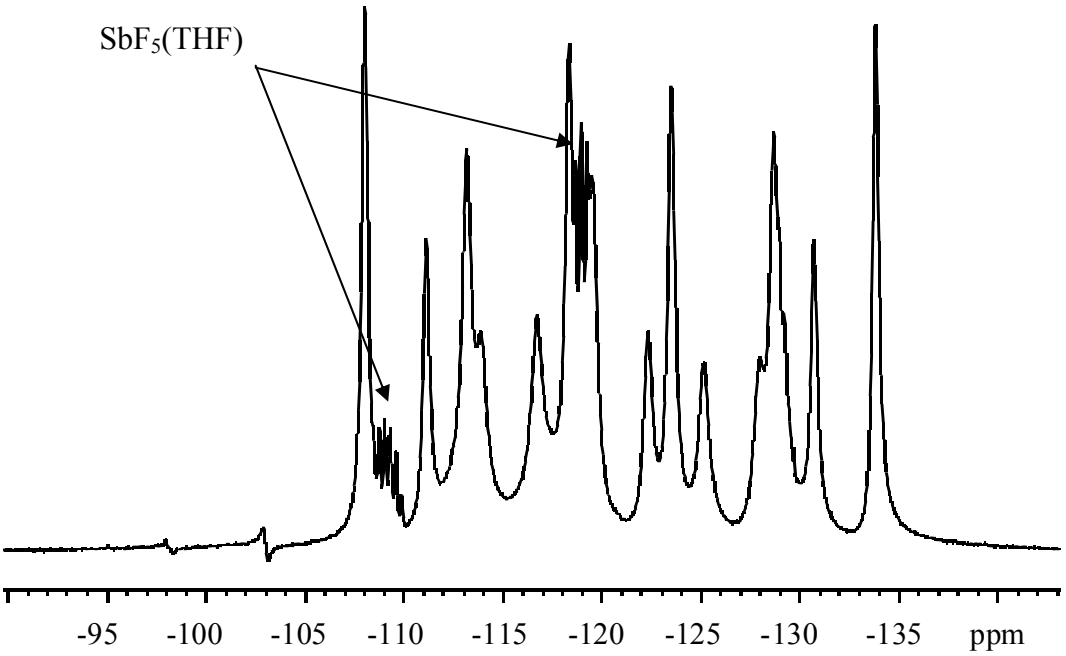

Figure 12.

^{19}F NMR spectrum of **[1]** with 10 equivalents of THF in MeCN at -40 ºC, in the region of the Sb-F resonances. The ^{19}F NMR shows the signal of the $[SbF_6]^-$ anion overlapping with the resonances assigned to the SbF_5(THF). This spectrum is measured 3 hours after preparation of solution.

NMR scale Experiment. Reaction of [TiF$_3$(MeCN)$_3$][SbF$_6$]·MeCN [1] and THF in MeCN: 0.03 ml (0.031g, 0.42 mmol) of THF and 0.5 ml of MeCN were added to **[1]** (0.10 g, 0.20 mmol) in an 5 mm NMR tube. A clear colorless solution was obtained. The NMR spectra were measured 2-4 hours after preparation. ^{1}H NMR (400 MHz, MeCN, -40 ºC), δ_H (ppm) = 4.6 (4H, THF in complex), 4.4 (4H, THF in complex), 4.3 (4H, *cis*-TiF_4(THF)$_2$), 4.0 (4H, THF in complex), 3.3 (4H, THF), 2.7 (4H, THF in complex), 2.4 (4H, THF in complex), 2.3 (4H, THF in complex), 2.1 (4H, *cis*-TiF_4(THF)$_2$), 2.1 (MeCN), ^{19}F NMR (MeCN, -40 ºC), δ_F (ppm) = 320.0 (s, *face* - [TiF_3(MeCN)$_3$]$^+$), 309.1 (2F, *cis* - [TiF_3(MeCN)$_2$(THF)]$^+$), 298.0 (1F, *cis* - [TiF_3(MeCN)(THF)$_2$]$^+$), 296.5 (1F *cis* - [TiF_3(MeCN)$_2$(THF)]$^+$), 285.6 (2F, *cis* - [TiF_3(MeCN)(THF)$_2$]$^+$), 281.9 (*face* - [TiF_3(THF)$_3$]$^+$), 237.1, 234.5, 230.8, 227.9, 225.2, 223.8, 222.9, 219.1, 217.6, 215.4 (2F *cis* - TiF_4(THF)$_2$), 214.1, 212.3, 210.1, 208.5, 206.3, 202.4,

181.2, 176.7, 169.1, 167.0, 162.4 (2F *cis* - TiF_4(THF)$_2$), -109 SbF_5(THF)), -119 (SbF_5(THF)), -121 (m, 6F, [SbF_6]$^-$ J(^{121}Sb-^{19}F) 1934 Hz, J(^{123}Sb-^{19}F) 1038 Hz). Resonances δ_F 237.1-202.4 and 181.2-167.0 are very weak, only the resonance at 217.6 ppm has considerable relative intensity.

[TiF$_3$(MeCN)$_3$][SbF$_6$]·MeCN [1] with 10 moles of THF in MeCN: 4.6 (4H, THF in complex), 4.5 (4H, THF in complex), 4.3 (4H, THF in complex), 4.2 (4H, THF in complex), 4.1 (4H, *cis*-TiF_4(THF)$_2$), 4.0 (4H, THF in complex), 3.6 (4H, THF), 1.9 (MeCN), 1.7 (4H, THF), ^{19}F NMR (MeCN, -40 ºC), δ_F (ppm) = 281.9 (*face* - [TiF_3(THF)$_3$]$^+$, 14%), 218.1 (30%), 216.1 (2F *cis* - TiF_4(THF)$_2$, 24%), 181.3 (1%), 167.6 (10%), 162.8 (2F *cis* - TiF_4(THF)$_2$, 21%), -109 (SbF_5(THF)), -119 (SbF_5(THF)), -121 (m, 6F, [SbF_6]$^-$ J(^{121}Sb-^{19}F) 1934 Hz, J(^{123}Sb-^{19}F) 1038 Hz). Spectrum was measured 2-3 hours after preparation.

The ^{19}F NMR spectra and color (colorless to yellow) changed with time.

[TiF$_3$(MeCN)$_3$][SbF$_6$]·MeCN [1] with 10 moles of THF in MeCN, measured 10 days after preparation: 4.6 (4H, THF in complex), 4.2 (4H, THF in complex), 4.0 (4H, *cis*-TiF_4(THF)$_2$), 3.9 (4H, THF in complex), 3.5 (4H, THF), 3.2 (br), 1.9 (MeCN), 1.7 (4H, THF), ^{19}F NMR (MeCN, -40 ºC), δ_F (ppm) = 213.9 (2F *cis* - TiF_4(THF)$_2$, 37%), 205.2 (1%), 179.1 (1%), 166.4 (1%), 165.4 (26%), 160.5 (2F *cis* - TiF_4(THF)$_2$, 32%), -112.5 -109 (SbF_5(THF)), -121.5 (SbF_5(THF)), -123 (br, [SbF_6]$^-$). Deposition of solid product was not observed from the reaction mixture, the residue obtained on evacuation of the volatile products was a yellow oil.

7. Reaction of [1] and excess of H_2O in MeCN.

Interaction of **[1]** with 1-3 equivalent of H_2O in MeCN was studied by means of NMR spectroscopy.

The ^{19}F NMR spectrum of a solution of **[1]** with 1-3 moles of H_2O in MeCN at -40 ºC contains the resonances due to *face*-$[TiF_3(MeCN)_{3-n}(H_2O)_n]^+$ n = 0 - 3, the relative intensity of which depends on the ratio of **[1]** to H_2O (Figure 13.). The proton spectrum contains resonance at 11.6 ppm, in the area of resonances due to protons of the RCOO*H* and RSO_3H groups [12] as well as resonances at 2.83, 2.79, 2.51 ppm of the coordinated MeCN, showing that coordinated H_2O in the titanium cationic complexes is acting as a Brønsted acid and confirming the presence of the complexes containing MeCN ligands. The signals δ_F 215.8, 146.3 ppm were assigned to the *cis*-$TiF_4(H_2O)_2$ by comparison with previous work [13], the broad signal at 159 ppm probably arises from the mixed complex *cis*-$TiF_4(MeCN)(Et_2O)$. Resonances at 234.1, 232.4, 224.2, 223.6, 221.9, 219.5, 217.0, 208.5, 204.9 ppm were attributed to titanium fluoride complexes containing bridging and terminal $[OH]^-$ and $[O]^{2-}$ ligands. Transformations of the coordinated water into $[OH]^-$ and the $[O]^{2-}$ ligands were observed in the related systems TaF_5 – H_2O [14,15], TiF_4 – H_2O [16]. The NMR spectra of these solutions showed resonances of monomeric and oligomeric fluoride complexes containing the terminal and bridging $[OH]^-$ as well as $[O]^{2-}$ ligands.

The ^{19}F NMR spectra of **[1]** with H_2O contained a signal resonance attributable to that of the $[SbF_6]^-$ anion overlapping with the resonances of antimony fluoride complexes (Fig.8) resulting from hydrolysis of $[SbF_6]^-$. The relative concentration of the mixed antimony complexes decreases with the time (see lower spectrum (Figure 14.)).

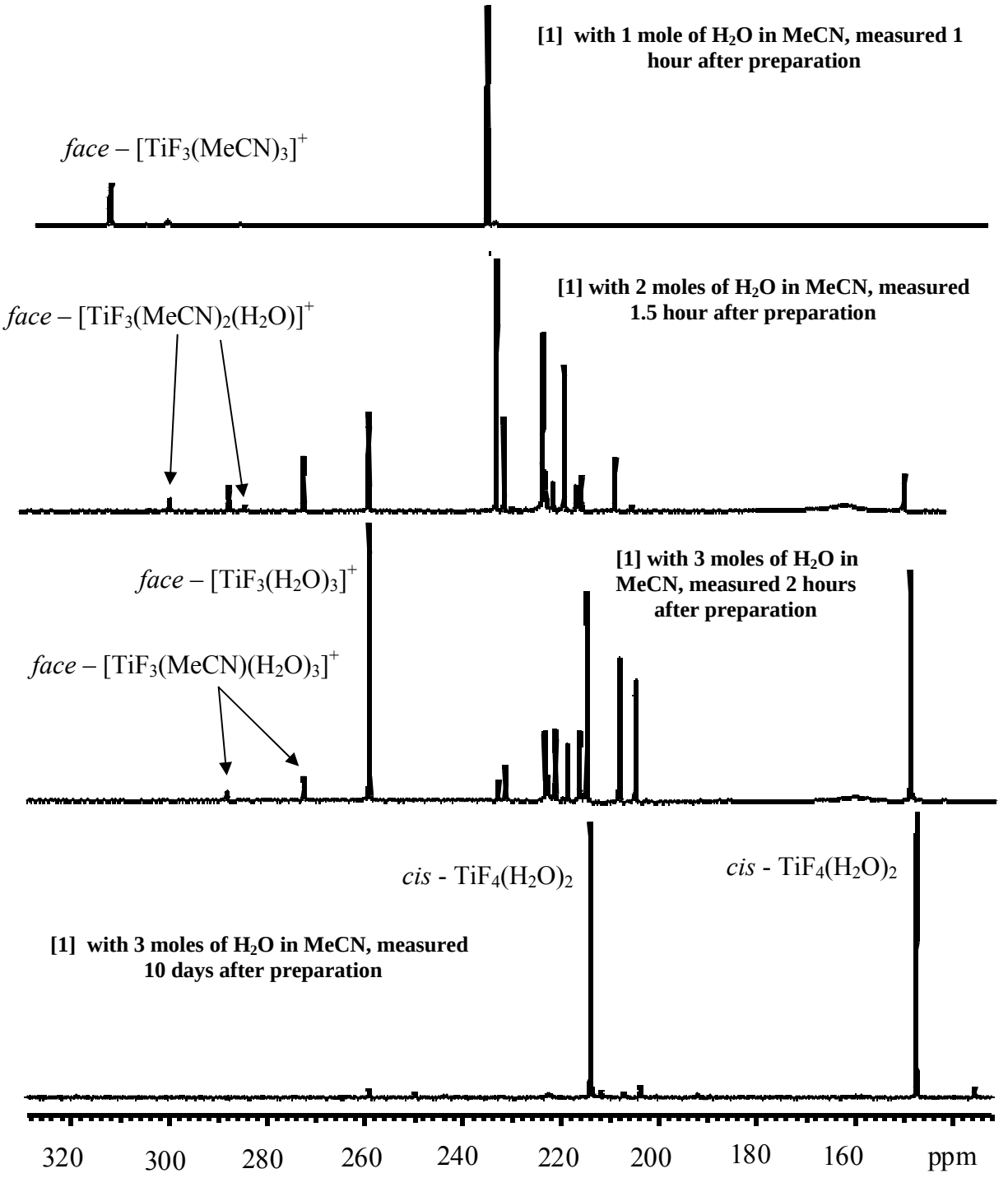

Figure 13.

Upper three spectra: ^{19}F NMR spectrum of **[1]** with 1-3 equivalents of H_2O in MeCN, -40 ºC, measured 1, 1.5 and 2 hours after preparation.
Lower spectrum: **[1]** with 3 equivalents of H_2O in MeCN, -40 ºC is measured 10 days after preparation.

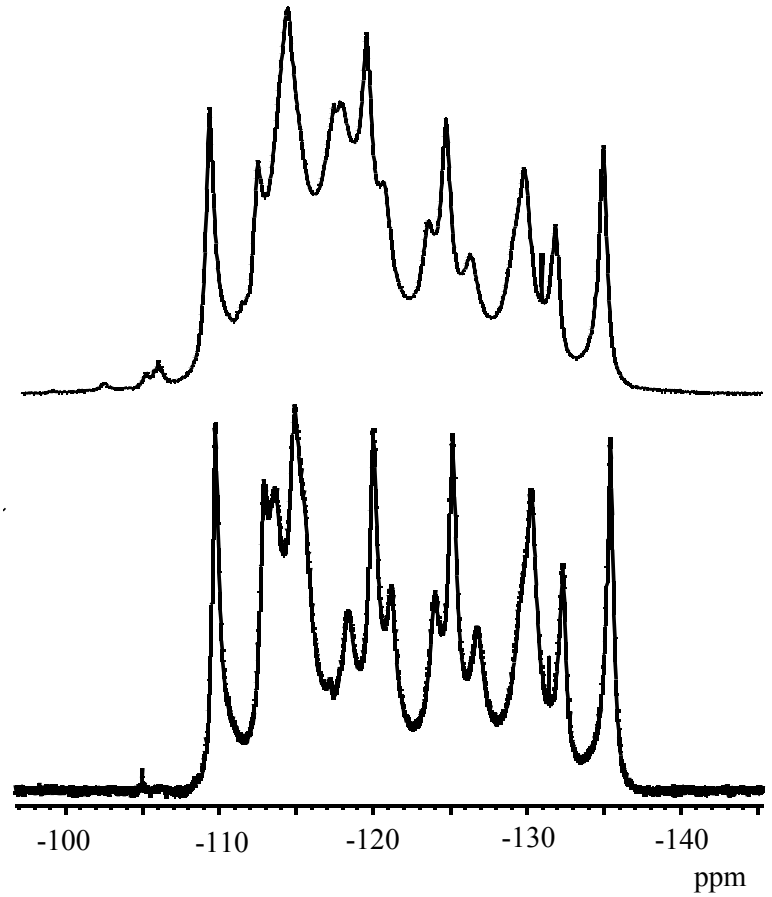

Figure 14.

^{19}F NMR spectrum of **[1]** with 3 equivalents of H_2O in MeCN at -40 ºC in the region of the Sb-F resonances. The top spectrum is measured 3 hours after preparation of solution, the bottom spectrum is measured 9 days after preparation of solution. The relative amount of the mixed antimony fluoride complexes is seen to decrease with the time.

A white powder was slowly deposited from a solution of **[1]** with 3 equivalents of H_2O in MeCN at r.t. The relative intensity of cationic complexes decreased with the time due to decomposition in solution accompanied by formation of oligomeric complexes containing $[OH]^-$ and $[O]^{2-}$ terminal and bridging ligands. A ^{19}F NMR spectrum recorded 10 days after preparation of solution mainly contains signals of *cis* - $TiF_4(H_2O)_2$ and $[SbF_6]^-$ (Figure 13., Figure 14.). The proton spectrum recorded at the same time contained several strong broad signals in the region 10.6 – 8.8 ppm as well as the resonance of the *cis* - $TiF_4(H_2O)_2$ at 7 ppm.

NMR scale Experiment. Reaction of [$TiF_3(MeCN)_3$][SbF_6]·MeCN [1] with H_2O in MeCN: 0.6 ml of MeCN was condensed onto **1** (0.1 g, 0.2 mmol) in an 5 mm NMR tube. A clear colorless solution was obtained by warming. By means of a micro syringe three aliquots of H_2O $3.5 \cdot 10^{-3}$ ml each were added. The NMR spectra were measured of 3-4 hours after preparation.

*[$TiF_3(MeCN)_3$][SbF_6]·MeCN (**1**) and 1 equivalent of H_2O in MeCN:* ^{1}H NMR (400 MHz, MeCN, -40 ºC), δ_H (ppm) = 11.6 (br), 2.83 (MeCN in complex), 2.79 (MeCN in complex), 2.70 (MeCN in complex), 2.3 (MeCN solvent); ^{19}F NMR (MeCN, -40 ºC), δ_F (ppm) = 317.3 (3F *face*-[TiF_3(MeCN)$_3$]$^+$), 304.7 (2F *face*-[TiF_3(MeCN)$_2$(H_2O)]$^+$), 288.7 (1F *face*-[TiF_3(MeCN)$_2$(H_2O)]$^+$), 234.2 (br), -107.5 (br), -114.8 ((H_2O)SbF_5), -123.3 (m, 6F, [SbF_6]$^-$ J(^{121}Sb-^{19}F) 1942 Hz, J(^{123}Sb-^{19}F) 1049 Hz).

Reaction of [1] with 2 equivalents of H_2O in MeCN: ^{1}H NMR (400 MHz, MeCN, -40 ºC), δ_H (ppm) = 10.9 (br), 8.7 (br), 8.4 (br), 8.1 (br), 7.8 (br), 3.2 (MeCN in complex), 2.9 (MeCN in complex), 2.7 (MeCN in complex), 2.3 (MeCN solvent); ^{19}F NMR (MeCN, -40 ºC), δ_F (ppm) = 304.5 (2F *face*-[TiF_3(MeCN)$_2$(H_2O)]$^+$), 291.7 (1F *face*-[TiF_3(MeCN)(H_2O)$_2$]$^+$), 288.7 (1F *face*-[TiF_3(MeCN)$_2$(H_2O)]$^+$), 275.7 (2F *face*-[TiF_3(MeCN)(H_2O)$_2$]$^+$), 261.7 (3F *face*-[TiF_3(H_2O)$_3$]$^+$), 234.1 (br), 232.4 (br), 224.2 (br), 223.6 (2F, *cis*-TiF_4(H_2O)(MeCN)), 221.9 (br), 219.5 (br), 217.0 (br), 215.8 (2F, *cis* - TiF_4(H_2O)$_2$), 208.5 (br), 159 (*cis*-TiF_4(H_2O)(MeCN)), 146.3 (*cis* - TiF_4(H_2O)$_2$). -102 (d, J = 72 Hz, (H_2O)SbF_5), -106.0 (t, J =93 Hz,), -123.3 (m, 6F, [SbF_6]$^-$ J(^{121}Sb-^{19}F) 1940 Hz, J(^{123}Sb-^{19}F) 1048 Hz).

Reaction of [1] with 3 equivalents of H_2O in MeCN: ^{1}H NMR (400 MHz, MeCN, -40 ºC), δ_H (ppm) = 10.0 (br), 8.4 (br), 8.1 (br), 7.8 (br), 7.6 (br), 3.2 (MeCN in complex), 2.9 (MeCN in complex), 2.8 (MeCN in complex), 2.7 (MeCN in complex), 2.3 (MeCN solvent); ^{19}F NMR (MeCN, -40 ºC), δ_F (ppm) = 291.4 (1F, *face*-[TiF_3(MeCN)(H_2O)$_2$]$^+$), 275.0 (2F, *face*-[TiF_3(MeCN)(H_2O)$_2$]$^+$), 261.3 (3F, *face*-[TiF_3(H_2O)$_3$]$^+$), 234.0 (br), 232.4 (br), 224.1 (br),

223.5 (2F, *cis*-TiF_4(H_2O)(MeCN)), 221.8 (br), 219.2 (br), 216.7 (br), 215.1 (2F, *cis* - TiF_4(H_2O)$_2$), 208.3 (br), 204.8 (br), 159 (*cis*-TiF_4(H_2O)(MeCN)), 146.8 (*cis* - TiF_4(H_2O)$_2$). – 102.8 (d, J = 69 Hz, (H_2O)SbF_5), -105.6 (br), -106.3 (t, J = 91 Hz,), -114.8, -120.0, -123.3 (m, 6F, [SbF_6]$^-$ J(^{121}Sb-^{19}F) 1943 Hz, J(^{123}Sb-^{19}F) 1046 Hz).

Reaction of [1] with 3 equivalents of H_2O in MeCN, measured after 10 days: ^{1}H NMR (400 MHz, MeCN, -40 ºC), δ_H (ppm) = 10.6 (br), 9.5 (br), 9.0 (br), 8.8 (br), 7.6 (br), 7.5 (br), 7.0 (*cis* - TiF_4(H_2O)$_2$), 2.3 (MeCN solvent); ^{19}F NMR (MeCN, -40 ºC), δ_F (ppm) = 259.1 (3F, *face*-[TiF_3(H_2O)$_3$]$^+$), 249.7 (br), 243.5 (br), 223.5 (br), 211.8 (*cis* - TiF_4(H_2O)$_2$), 207.1 (br), 203.7 (br), 147.3 (*cis* - TiF_4(H_2O)$_2$), 135.5 (br), -113.6 (br), -122.5 (m, 6F, [SbF_6]$^-$ J(^{121}Sb-^{19}F) 1950 Hz, J(^{123}Sb-^{19}F) 1053 Hz) the total relative intensity of resonances of *cis* - TiF_4(H_2O)$_2$ is 90%.

7. "Volume-Based" Thermodynamics (VBT) applied to the studied systems.

Ion volumes can be regarded as being additive and thus we can use the resource of our database of ion volumes with the cation volumes in Table 6 to estimate thermodynamic parameters for other complex salts (real and hypothetical). Thus, for example, the hypothetical salt [*face*-TiF_3(MeCN)$_3$][AsF_6] would be estimated to have a volume given by:

V_m ([*face*-TiF_3(MeCN)$_3$][AsF_6]) = V[*face*-TiF_3(MeCN)$_3$]$^+$ + V[AsF_6]$^-$ (1)

and since the latter V[AsF_6]$^-$ has a value 0.110 (± 0.012)nm^3 [17] and the former (Table 6, ESI) a value of 0.278 (± 0.012) nm^3, then

V_m ([*face*-TiF_3(MeCN)$_3$][AsF_6]) ≈ 0.388 (± 0.012) nm^3 (2)

and hence the corresponding estimated thermodynamic parameters:

U_{POT}([*face*-TiF_3(MeCN)$_3$][AsF_6]) ≈ 425 (± 3) kJ mol^{-1} (3)

S^0_{298}([*face*-TiF_3(MeCN)$_3$][AsF_6]) ≈ 543 (± 16) J K^{-1} mol^{-1} (4)

Table 6.

Volumes of Complex Salts and Solvates derived from crystal structure data (or their estimated ion volumes) and the corresponding lattice potential energies and standard entropies at 298K.

Complex	**V(Complex) / nm^3**	**U_{POT} (Complex) / kJ mol^{-1}** **S^0_{298} (Complex) / J K^{-1} mol^{-1}**	**Notes**
[*face*-$TiF_3(MeCN)_3$][SbF_6]·MeCN (**1**)	1.7826 / 4 = 0.4457 [a]	See footnote [18]	[a] Table 6 main text [b] Eqn 2, α = 117.3 kJ mol^{-1} nm; β = 51.9 kJ mol^{-1}
[*face*-$TiF_3(MeCN)_3$][SbF_6][c]	0.4457 – 0.047 = 0.3987 [a]	423[b] 557[h]	[a] Subtraction of solute volume, *V*(MeCN)[e] [b] Eqn 2, α = 117.3 kJ mol^{-1} nm; β = 51.9 kJ mol^{-1}
[TiF_2(15-Crown-5)][SbF_6]$_2$ (**2**)	1.08516 / 2 = 0.5426 [a]	1348[b] 753[h]	[a] Table 6 main text [b] Eqn 2, α = 133.5 kJ mol^{-1} nm; β = 60.9 kJ mol^{-1}
[TiF_2(18-Crown-6)][SbF_6]$_2$ (**3**)	1.1704 / 2 = 0.5852 [a]	1323 [b] 811[h]	[a] Table 6 main text [b] Eqn 2, α = 133.5 kJ mol^{-1} nm; β = 60.9 kJ mol^{-1}
[$TiCl_3$(15-Crown-5)(MeCN)][$SbCl_6$][d]	2.690 / 4 = 0.6725 [a]	372[b] 930[h]	[a] Ref [19]. b Eqn 2, α = 117.3 kJ mol^{-1} nm; β = 51.9 kJ mol^{-1}
[$TiCl_3(MeCN)_3$][$SbCl_6$]	2.3749 / 4 = 0.5937 [a]	See endnote [20]	[a] Ref [21]
[18-Crown – 6]·2MeCN[f]	1.006031/2 = 0.5030 [a]	-	[a] Table 6 main text
[$TiF_3(SO_2)_3$][SbF_6]	0.4227[j]	416[b] 590[h]	Example of estimation of lattice energy of salt for which there is no crystal structure data available using isomegethic rule[j]
Ion	**V(Ion) / nm^3**	**-**	**Notes**
[*face*-$TiF_3(MeCN)_3$]$^+$	0.3987 – 0.121 (±0.012) = 0.278 (±0.012)	-	Subtraction of volume of counter anion from volume of complex c
[TiF_2(15-Crown-5)]$^{2+}$	0.5426 – 2{0.121 (±0.012)} = 0.301 (±0.017)	-	Subtraction of volume of counter anion from volume of complex (**2**)
[TiF_2(18-Crown-6)]$^{2+}$	0.5852 – 2{0.121 (±0.012)} = 0.343 (±0.017)	-	Subtraction of volume of counter anion from volume of complex (**3**)

$[TiCl_3(15\text{-Crown-5})(MeCN)]^+$	0.6725 – 0.121 (±0.012)} = 0.552 (±0.012)	-	Subtraction of volume of counter anion from volume of complex d

[e] No crystal structure data is available for MeCN in the *solid* state. However the solid compound acetonitrile mercury(II) bromide: $MeCN{\cdot}3HgBr_2$ (M = 1122.25) has a reported density [18(c)] of 5.48 g cm^{-3}, from which we can estimate that $V_m(CH_3CN{\cdot}3HgBr_2)$ = 0.340 nm^3. From crystal structure data [18(c)]: $V_m(MeCN{\cdot}3HgBr_2)$ = 1.4410 / 4 = 0.3602 nm^3, leading us to an average experimental value: $V_m(MeCN.3HgBr_2)$ = 0.350 ± 0.010 nm^3. The compound $HgBr_2$ (M = 760.40) has a reported experimental density of 5.73 g cm^{-3} leading to a volume, $V_m(HgBr_2)$ = 0.1044 nm^3; from crystal structure data we have: $V_m(HgBr_2)$ = 0.3912/ 4 = 0.0978 nm^3, averaging to $V_m(HgBr_2)$ = 0.101 ± 0.003 nm^3. Accordingly: $V_m(MeCN)$ = $[V_m(MeCN{\cdot}3HgBr_2) - 3\ V_m(HgBr_2)]$ = 0.047 ± 0.011 nm^3. [g] S^0_{298}(Complex) / J K^{-1} mol^{-1} ≈ 1360 V_m(Complex) + 15; [i] $V_m[TiF_3(SO_2)_3][SbF_6] \approx V_m([face\text{-}TiF_3(MeCN)_3]\ [SbF_6]) - 3V_m(MeCN) + 3V_m(SO_2)$; $V_m(SO_2)$ = 0.055 nm^3 from [22].

8. Lattice Energies: $U_{POT}([TiF_3][Sb_mF_{5m+1}])$

The lattice energies U_{POT} of the $[TiF_3][Sb_mF_{5m+1}]$ salts were calculated from equation (3) using experimentally determined volumes of the $[SbF_6]^-$ 0.121 (± 0.012) nm^3, $[Sb_2F_{11}]^-$ 0.227 (± 0.020) nm^3 and $[Sb_3F_{16}]^-$ 0.317 (± 0.021) nm^3 [17]. Volume of the $[TiF_3]^+ \approx$ 0.057 nm^3 was calculated using the Gaussian Program [23], since no structural information for $[TiF_3]^+$ salts is currently available and there are insufficient entries for Ti salts in our ion volume database to use the isomegethic rule [24] to estimate this volume. The calculated volume of $[TiF_3]^+$ was compared with the experimentally determined volumes of TiF_3 0.058 nm^3 [25], and sample

calculations were performed for (similar) ions whose volume is already known. Thus we found that: $V[SeF_3]^+$ was calculated to be 0.05 nm^3, whilst the database entry was 0.053 (±0.007) nm^3 [17] and similarly: $V[SF_3]^+$ calcd. 0.061 nm^3, compared to the database 0.053 (±0.011) nm^3 [17, Table 6], therefore our approach to the estimation of $V[TiF_3]^+$ seems reasonable and is used for estimation of the lattice enthalpy in Scheme 4 of the main text.

Table 7. Definition of complexation reactions, ΔH_{comp} used in the cycle in main text (Scheme 4) and overall enthalpy change, $\Delta H_m^{'}$ for reaction:

$TiF_4L_2(s) + SbF_5L(s) + (m-1)SbF_5(l) \rightarrow [TiF_3L_3][Sb_{m+1}F_{5m+6}](s)$

Reaction	ΔH_{comp}(g)
TiF_4L_2 (g) → TiF_4 (g) + 2L (g)	- $\Delta H_{comp}(TiF_4L_2,g)$ = - enthalpy of complexation of TiF_4(g) = 2 $E(Ti–L)_{mol\ compl}$ = 2 x bond energy of Ti-L bond in TiF_4L_2
SbF_5L (g) → SbF_5 (g) + L (g)	- $\Delta H_{comp}(SbF_5L,g)$ = - enthalpy of complexation of SbF_5(g) = $E(Sb–L)_{mol\ compl}$ = bond energy of Sb-L bond in SbF_5L
$[TiF_3]^+$ (g) + 3L (g) → $[TiF_3L_3]^+$ (g)	$\Delta H_{comp}([TiF_3L_3]^+,g)$ = enthalpy of complexation of $[TiF_3]^+$(g) = - $3E(Ti–L)_{cat\ comp}$ = - 3 x bond energy of Ti-L bond in $[TiF_3L_3]^+$ ion.
Scheme 4, m = 1 $\Delta H_1^{'}$	$\Delta H_1^{'} = \Delta H_{sub}(TiF_4L_2,s) + \Delta H_{sub}(SbF_5L,s) + \Delta H_{comp}([TiF_3L_3]^+,g) + 633$ (± 18) - $\Delta H_{comp}(TiF_4L_2,g) - \Delta H_{comp}(SbF_5L,g) - U_{POT}([TiF_3L_3][SbF_6])$ = - $U_{POT}([TiF_3L_3][SbF_6]) + \Delta H_{comp}([TiF_3L_3]^+,g) + 633$ (± 18) – $\Delta H_{comp}(TiF_4L_2,s)$) – $\Delta H_{comp}(SbF_5L,s)$
Scheme 4, m = 2 $\Delta H_2^{'}$	$\Delta H_2^{'} = \Delta H_{sub}(TiF_4L_2,s) + \Delta H_{sub}(SbF_5L,s) + \Delta H_{comp}([TiF_3L_3]^+,g) + 509$ (± 25) – $\Delta H_{comp}(TiF_4L_2,g) - \Delta H_{comp}(SbF_5L,g) - U_{POT}([TiF_3L_3][Sb_2F_{11}])$ = - $U_{POT}([TiF_3L_3][Sb_2F_{11}]) + \Delta H_{comp}([TiF_3L_3]^+,g) + 509$ (± 25) – $\Delta H_{comp}(TiF_4L_2,s)$ – $\Delta H_{comp}(SbF_5L,s)$
Scheme 4, m = 3 $\Delta H_3^{'}$	$\Delta H_3^{'} = \Delta H_{sub}(TiF_4L_2,s) + \Delta H_{sub}(SbF_5L,s) + \Delta H_{comp}([TiF_3L_3]^+,g) + 434$ (± 31) – $\Delta H_{comp}(TiF_4L_2,g) - \Delta H_{comp}(SbF_5L,g)$ $U_{POT}([TiF_3L_3][Sb_3F_{16}])$ = - $U_{POT}([TiF_3L_3][Sb_3F_{16}]) + \Delta H_{comp}([TiF_3L_3]^+,g) + 434$ (± 21) – $\Delta H_{comp}(TiF_4L_2,s)$ – $\Delta H_{comp}(SbF_5L,s)$

[a] $\Delta H_{comp}(TiF_4L_2,g)$ corresponds to the process: $TiF_4(g) + 2L(g) \rightarrow TiF_4L_2(g)$; [b] $\Delta H_{comp}(SbF_5L,g)$ corresponds to the process: $SbF_5(g) + L(g) \rightarrow SbF_5L(g)$; [c] $\Delta H_{comp}(TiF_4L_2,s)$ corresponds to the process: $TiF_4(g) + 2L(g) \rightarrow TiF_4L_2(s)$; [d] $\Delta H_{comp}(SbF_5L,s)$ corresponds to the process: $SbF_5(g) + L(g) \rightarrow SbF_5L(s)$. Also: $\Delta H_{comp}(TiF_4L_2,g) = \Delta H_{comp}(TiF_4L_2,s) + \Delta H_{sub}(TiF_4L_2,s)$ and $\Delta H_{comp}(SbF_5L,g) = \Delta H_{comp}(SbF_5L,s) + \Delta H_{sub}(SbF_5L,s)$

To the best of our knowledge no thermodynamic values for the $[TiF_3L_3][SbF_6]$ salts or for TiF_4L_2 and SbF_5L adducts (L = SO_2, MeCN, THF, Et_2O, $(MeO)_3PO$, H_2O, Ph_3PO, Me_2SO and crown ethers) are to be found in the literature. However the newly reported "difference rule" [26] facilitates enormously the acquisition of estimates of data which would otherwise be unavailable, both for solvated and unsolvated salts. Table 8 (S.I.) illustrates the generation of such data and the assembled data which is estimated relies only on prior knowledge of only a small amount of data (i.e. Θ_{Hf}(L,s-s) values for L = SO_2, Et_2O and H_2O from reference [26]; the enthalpy of the reaction: $TiF_4{\cdot}2py(s) \rightarrow TiF_4(s) + 2\ py(g)$, determined experimentally [27] to be 46 kJ mol^{-1} and leading to $\Delta_f H^0(TiF_4{\cdot}2py,s)$ = -2325.2 kJ mol^{-1} and the known data for $\Delta_f H^0(TiF_4{\cdot}MeCN,s)$ [28]).

Table 8 Estimation of $\Delta H_{comp}(TiF_4L_2,s)$ and other thermodynamic data / kJ mol^{-1} using available data and the difference rule.

L	$\Delta_f H^0(TiF_4L_2,s)$	$\Delta_f H^0$(L,g)	$\Delta_f H^0(TiF_4,g)$	Θ_{Hf}(L,s-s)	$\Delta H^0_{comp}(TiF_4L_2, s)$[f]
SO_2	- 2325.2 [a]	- 296.8	- 1551	- 339.7 [b]	- 181
MeCN	- 1543.2 (± 10) [a]	64.3 (± 7.1)	- 1551	51.3 (± 7.1) [c]	-121 (± 10)
Et_2O	- 2210.0 [a]	- 184.1	- 1551	- 282.1 [b]	- 291
H_2O	- 2243.0 [a]	- 241.8	- 1551	- 298.6 [b]	- 208
py	- 1411 (± 7.1) [e]	140.4	- 1551	117.4[d]	- 141 (± 7)

[a] $\Delta H^0_{comp}(TiF_4L_2,\ s) = \Delta_f H^0(TiF_4L_2,s) - 2\Delta_f H^0(L,\ g) - \Delta_f H^0(TiF_4,s)$; [b] Reference [26] using $\Delta_f H^0(TiF_4,s)$ = - 1645.8 kJ mol^{-1}; [c] $\Theta_{Hf}(MeCN,\ s\text{-}s) = \Delta_f H^0(TiF_4{\cdot}MeCN,s) - \Delta_f H^0(TiF_4,s)$,

$\Delta_f H^0$(TiF_4·MeCN,s) = -1594.5 kJ mol^{-1} [28]; [d] Θ_{Hf}(py, s-s) = ½[$\Delta_f H^0$(TiF_4·2py,s) - $\Delta_f H^0$(TiF_4,s)]; [e] ΔH[TiF_4·2py(s) → TiF_4(s) + 2 py(g)] = 46 kJ mol^{-1} [27], $\Delta_f H^0$(TiF_4·2py,s) = $\Delta_f H^0$(TiF_4,s) + 2 $\Delta_f H^0$(py,g) - ΔH[TiF_4·2py(s) → TiF_4(s) + 2 py(g)].

We note from Table 8 that the estimated values for ΔH^0_{comp}(TiF_4L_2, s) take the order: MeCN > py > SO_2 > H_2O > Et_2O. ΔH^0_{comp}(SbF_5·L,s) corresponds to the process: SbF_5(g) + L(g) → SbF_5L (s) and is given by:

$$\Delta H^0_{comp}(SbF_5\cdot L,s) = \Delta_f H^0(SbF_5\cdot L,s) - \Delta_f H^0(SbF_5,g) - \Delta_f H^0(L,g)$$
$$= \Delta_f H^0(SbF_5\cdot L,s) + 1301\ (\pm 15) - \Delta_f H^0(L,g) \qquad (5)$$

In the case where L = SO_2, from previous work [29] we know that $\Delta_f H^0$(AsF_5·SO_2,s) = - 1565 kJ mol^{-1} and therefore using the difference rule [26, $P = \Delta_f H^0$] we find that:

$$\Theta_{Hf}(SO_2,\ s\text{-}g) / kJ\ mol^{-1} = \Delta_f H^0(AsF_5\cdot SO_2,s) - \Delta_f H^0(AsF_5,g) = -328 \qquad (6)$$

We can, since $\Delta_f H^0$(SbF_5,g) = - 1301 (±15) kJ mol^{-1}, conjecture that:

$$\Delta_f H^0(SbF_5\cdot SO_2,s) / kJ\ mol^{-1} \approx -1629 \qquad (7)$$

and hence that:

$$\Delta H^0_{comp}(SbF_5\cdot SO_2,s) / kJ\ mol^{-1} \approx -31.2 \qquad (8)$$

For a general solvent, L:

$$\Delta_f H^0(SbF_5\cdot L,s) - \Delta_f H^0(SbF_5,g) = \Theta_{Hf}(L,\ s\text{-}g) \qquad (9)$$

and since only Θ_{Hf}(L, s-s) values are available (Table 7) the remaining values required cannot at this stage be estimated. In the case where L = SO_2 however, we can calculate $\Delta_1 H'$(s) (equation (9) in the text, m = 1, L = SO_2 and table 8) to be:

$\Delta_1 H^{'}$(s) / kJ mol^{-1} = $\Delta H_{comp}([TiF_3(SO_2)_3]^+,g)$ – (-181)-(-31.2) – (471)

$= \Delta H_{comp}([TiF_3(SO_2)_3]^+,g)$ - 258.8 (10)

where $U_{POT}([TiF_3(SO_2)_3][SbF_6])$ is estimated in Table 6 (row 8). The value of $\Delta H_{comp}([TiF_3(SO_2)_3]^+,g)$, corresponds to the process: $[TiF_3]^+(g) + 3\ SO_2(g) \rightarrow [TiF_3(SO)_3]^+(g)$

So that:

$\Delta_1 H^{'}$(s) / kJ mol^{-1} = $\Delta_f H^0([TiF_3(SO)_3]^+g) - 3\ \Delta_f H^0(SO_2,g) - \Delta_f H^0([TiF_3]^+,g)$ - 258.8

$= \Delta_f H^0([TiF_3(SO)_3]^+g)$ + 476 > 0 (11)

This prediction is anticipated from our experimental findings in the main paper and the theory thus accords with expectations. Possession of an absolute value for $\Delta_f H^0([TiF_3(SO)_3]^+g)$ would then enable precise quantification of $\Delta_1 H^{'}$(s) / kJ mol^{-1}.

References and Notes

[1] (*a*) I.D. Brown, *Structure and Bonding in Crystals*, eds. M.O'Keefe, A. Navrotsky, Academic Press, London, 1981. (*b*) Values used: Sb(+5)-F(-1) R_o=1.797, B=0.37.

[2] (*a*) J.F. Lehmann, D.A. Dixon, G.J. Schrobilgen, *Inorg. Chem.* 2001, **40**, 3002. (*b*) More than 500 structures containing $[SbF_6]^-$ are deposited in the crystallographic database CCDC.

[3] (*a*) A. Bondi, *J.Phys. Chem*., 1964, **68**, 441. (*b*) N.L. Allinger, J.A. Hirsch, M.Ann Miller, I.J. Tyminski, F.A. Van Catledge, *J. Am. Chem. Soc.*, 1968, **90**, 1199.

[4] G. Herzberg, *Molecular spectra and molecular structure, 2. Infrared and Raman spectra of polyatomic molecules*, 2nd ed., New York, Toronto, D. Van Nostrand, 1950, p. 332.

[5] A. Vij, W. W. Wilson, V. Vij, F. S. Tham, J. A. Sheehy, K. O. Christe, *J. Am. Chem. Soc.* 2001, **123***,* 6308.

[6] (*a*) H. Takeuchi, T. Arai, I. Harada, *J. Molecular structure*, 1986, **146**, 197. (*b*) H. Sato, Y. Kasumoto, *Chem. Lett*., 1978, 635. (*c*) SDBSWeb: http://www.aist.go.jp/RIODB/SDBS/ (access date 18.07.2004).

[7] E. G. Il'in, G. B. Nikiforov, M. E. Ignatov, Yu. A. Buslaev. *Doklady Chemistry*,1999, **369**, 299.

[8] G.B. Nikiforov, S.G. Sakharov, E.G. Il'in, Ju.A. Buslaev, *Rus. J. Inorg. Chem*., 2001, **46**, 1045.

[9] (*a*) P.A.W. Dean., *Can. J. Chem*., 1973, **51**, 4024. (*b*) J. Pauli, W. Storek, L. Riesel, *Z. Chem*., 1988. **H.6**., B. 226.

[10] (*a*) D. M. Byler, D. F. Shriver, *Inorg. Chem.*, 1976, **15**, 32. (*b*) J. Bacon, P.A.W. Dean, R. J. Gillespie, *Can. J. Chem*., 1969, **47**, 1655.

[11] (*a*) J.Bacon, P.A.W. Dean, R. J. Gillespie, *Can. J. Chem*., 1970, **48**, 3413.(*b*) R.J. Gillespie, K.C. Moss, *J. Chem. Soc. (A)*, 1966, 1170.

[12] J. Mason, *Multinuclear NMR*; Plenum Press, New York, 1987, p.173.

[13] T.S. Cameron, A. Decken, E.G. Ilyin, G.B. Nikiforov, J. Passmore, *Eur. J. Inorg. Chem*., 2004 (in press).

[14] A.A. Vashman, A.N. Zozulin, E.G. Ilyin, Yu. A. Buslaev, *Doklady akademii Nauk*, 1994, **335**, 597.

[15] N.G. Furmanova, I.A. Verin, A.N. Zozulin, E.G. Ilyin, *Doklady akademii Nauk*, 1992, **37**, 136.

[16] Yu. A. Buslaev, D.S. Dyer, R.O. Ragsdale, *Inorg. Chem.*, 1967, **6**, 2208.

[17] H.D.B. Jenkins, H.K. Roobottom, J. Passmore, L. Glasser, *Inorg. Chem*., 1999, **38**, 3609.

[18] (*a*) For the salt: [*face*-$TiF_3(MeCN)_3$][SbF_6]·MeCN (**1**), being a *solvate* of MeCN, equation(2) does not apply. Accordingly, substitution of V_m([*face*-$TiF_3(MeCN)_3$][SbF_6]) into (2) *will not lead to* a correct estimate for U_{POT}([*face*-$TiF_3(MeCN)_3$][SbF_6]) (See scheme 3, ref [49b]). Instead, for solvates, the thermodynamic "difference rule" should be used to estimate lattice energies of solvated salts [26] from the parent (unsolvated) salt lattice energy. Thus:
U_{POT}([*face*-$TiF_3(MeCN)_3$][SbF_6].MeCN) = U_{POT}([*face*-$TiF_3(MeCN)_3$][SbF_6]) + + Θ_U(MeCN, s-s)
provided the constant Θ_U(MeCN, s-s) is known, U_{POT}([*face*-$TiF_3(MeCN)_3$][SbF_6]. MeCN) can be estimated. In this particular instance, however, although the volume of the parent salt can be obtained by estimation of V(MeCN) ([18(c)], because the constant, Θ_U(MeCN, s-s) is currently undetermined we cannot proceed to estimate the solvate lattice energy. Because the literature records a value for $\Delta_f H^0$(TiF_4·MeCN,s) and $\Delta_f H^0$(TiF_4,s) is also known a value for Θ_{Hf}(MeCN, s-s) can however be estimated (see text). (b) H. D. B. Jenkins, L. Glasser,. *Inorg. Chem*, 2002, **41**, 4378. (*c*) Landolt-Bornstein. Numerical Data and Functional Relationships in Science & Technology. New Series. Hellewege, K- H; Madelung, O. Eds/ Group III, Crystal and SolidState Physics. Volume 10. Structure Data of Organic Compounds. Subvolume a: C_1….C_{15}. Entry 102, Springer-Verlag, Heidelberg, 1979.

[19] M. Plate, G. Frenzen, K. Dehnicke, *Z. Naturforsch*., 1993, **48b**, 149.

[20] D. R. Lide, (Ed)., Handbook of Chemistry 7 Physics, 79th edition, C. R. C. Press, Boca Raton, FL, 1998.

[21] P.P.K. Claire, G.R. Willey, M.G.B. Drew, *Chem. Comm*., 1987, **14**, 1100.

[22] (b) J. D. H. Donnay and H. M. Ondik, *Crystal Structure Determinative Tables*, 3rd Edn. U. S. Department of Commerce, N. B. S. 1973.

[23] (*a*) The $[TiF_3]^+$ was optimised at the HF/6-311+G* level followed by MPW1PW91/6-311+G*, C_1 symmetry and singlet ground state.
M. J. Frisch, G. W. Trucks, H. B. Schlegel, G. E. Scuseria, M. A. Robb, J. R. Cheeseman, V. G. Zakrzewski, J. A. Montgomery, Jr., R. E. Stratmann, J. C. Burant, S. Dapprich, J. M. Millam, A. D. Daniels, K. N. Kudin, M. C. Strain, O. Farkas, J. Tomasi, V. Barone, M. Cossi, R. Cammi, B. Mennucci, C. Pomelli, C.

Adamo, S. Clifford, J. Ochterski, G. A. Petersson, P. Y. Ayala, Q. Cui, K. Morokuma, D. K. Malick, A. D. Rabuck, K. Raghavachari, J. B. Foresman, J. Cioslowski, J. V. Ortiz, B. B. Stefanov, G. Liu, A. Liashenko, P. Piskorz, I. Komaromi, R. Gomperts, R. L. Martin, D. J. Fox, T. Keith, M. A. Al-Laham, C. Y. Peng, A. Nanayakkara, C. Gonzalez, M. Challacombe, P. M. W. Gill, B. Johnson, W. Chen, M. W. Wong, J. L. Andres, C. Gonzalez, M. Head-Gordon, E. S. Replogle, J. A. Pople, Gaussian, Inc., Pittsburgh PA, USA, 1998.

[24] H. D. B. Jenkins, L. Glasser, T. M. Klapotke, M.-J. Crawford, K. K. Bhasin, J. Lee, G. J. Schrobilgen, L. S. Sunderlin, J. F. Liebman, *Inorg. Chem*., 2004, **43**, 6238.

[25] P. Ehrlich, G. Pietzka, *Z. Anorg. Allg. Chem*., 1954, **275***,* 121.

[26] H. D. B. Jenkins, L. Glasser, *J. Am. Chem. Soc,* 2004, **126**, 15809.

[27] H.J. Emeleus, G.S. Rao, *J. Chem. Soc*., 1958, 4245;
$\Delta H6(TiF_4L_2)$ (g) = -(138- ΔHsubl.(TiF_4Py_2)) kJ·mol-1, ΔHsubl.$(TiHal_4(Py)_2)$ was proposed to be approximately the same value for the $TiHal_4L_2$ Hal = F, Cl, L = molecular ligand.

[28] (*a*) L.V. Gurvich, I.V. Veyts, C.B. Alcock, *Thermodynamic Properties of individual substances*; Hemisphere Publishing Corporation, NY, 1989. (*b*) Thermodynamic Database: http://www.chem.msu.su/cgi-bin/tkv2.pl. (*c*) I.N. Bakulina, N.I. Ionov, *Rus J. Phys. Chem*., 1959, **33**, 2063.

[29] H. D. B. Jenkins, H. K. Roobottom, J. Passmore, *Inorg. Chem*., 2003, **42**, 2886.